Terremoti probabili in Italia dal 2000 al 2030: elementi per la definizione di priorità per la riduzione del rischio sismico

Coordinators: Alessandro Amato and Giulio Selvaggi

Task 3.2 "Local Geology Effect on Seismic Hazard"

Coordinators: Giovanna Cultrera, Antonio Rovelli
Working group: Paola Bordoni, Valerio De Rubeis, Fawzi Doumaz, Lucia Luzi, Lucia Margheriti, Fabrizio Marra, Marco Moro, Diego Sorrentino, Patrizia Tosi

Index

Task 3.2 "Local Geology Effect on Seismic Hazard"

Coordinators: Giovanna Cultrera, Antonio Rovelli
Working group: Paola Bordoni, Valerio De Rubeis, Fawzi Doumaz, Lucia Luzi, Lucia Margheriti, Fabrizio Marra, Marco Moro, Diego Sorrentino, Patrizia Tosi

The main purpose of Task 3.2 was to introduce the role of local geology in the seismic hazard evaluation at national scale. This was achieved by grouping the geological formation of the 1:500,000 Italian geological map into three classes A, B, C according to the EuroCode8 provisions (GCM, Geological-Class Map). These classes are associated to a variation of the ground motion due to the different seismic properties of the lithologies included in each group (ANNEX 1).
For a critical evaluation of the proposed approach, we have checked the occurrence of a systematic increment of macroseismic intensity as a function of the geological classes at a national scale. The study of distribution of Intensity anomalies associated to the 3 classes show a statistical significant tendency of positive anomalies to be related to classes B and C and negative anomalies to be related to class A (ANNEX 2).

We then assumed that the effect of local geology on ground motion is the one described by variation of elastic response spectra prescribed by EC8 (in terms of PGA, PSA, Housner Intensity). This variation is controlled by a set of parameters depending on the soil classes and earthquake magnitude (ANNEX 3).
We compared the increment factors to those deriving from a numerical simulation of the Città di Castello (Central Italy) basin where many geological and seismological data were available. The results at local scale show a good fit (within a factor of two) with the variations of hazard parameters for classes B e C (ANNEX 4).

Moreover, we launched a national-scale enquiry over the 8101 Italian Municipalities whose main goal was the estimation of the buildings distribution on the three soil classes corresponding to those of the CGM. We collected and organized the received forms in a database (see product 3). The comparison at a Municipality-scale of the GCM and the questionnaire results shows that their information is complementary, the first referring this percentage to the housing, the latter considering all the municipality territory (ANNEX 5). The questionnaire is a good data gathering tool for pointing out area where more detailed microzonation investigation must be performed. The questionnaire can be a powerful tool to increase awareness of Municipality Administration and the lack of involvement could be overcome by coordination at the Region levels.

Products

1. National geologic map at 1:500,000 scale modified according to the EC8 soil classes (geological-class map, GCM)
2. Map of the geology-dependent correction of hazard parameters
3. Database of the Italian municipalities containing information about the distribution of buildings in relation to the surface geology as well as geographical and geotechnical data availability.

The three products are organized in an attached CD and they are included in the GIS of the project.

ANNEX 1. Geological-Class Map (GCM)

Paola Bordoni, Fabrizio Marra, Marco Moro, Lucia Luzi, Lucia Margheriti

The outcropping formations of the 1:500,000 Italian geological map (Servizio Geologico Nazionale,1978) have been grouped into the three classes A, B, C according to the EuroCode8 provisions, EC8, after Draft 4 of December 2001 (ENV 1998). For the classification we have followed lithological and age criteria as in Table 1. Figure 1 maps the resulting Geological-Class Map (GCM).

Class	Description
A (rock) Vs > 800 m/s	Marine clay (Lower Pleistocene and Pliocene) and older rock (Paleogenic, Neogenic, Mesozoic and Paleozoic rocks). All of the volcanic rock and deposits (the original legend has not enough detail to allow finer distinction)
B (stiff soil) 400 < Vs < 800 m/s	Colluvial, alluvial, lacustrine, beach, fluvial terraces, glacial deposits, and clay (Middle-Upper Pleistocene.) Sand and loose conglomerate (Pleistocene and Pliocene). Travertine (Pleistocene and Holocene)
C (soft soil) Vs < 400 m/s	Colluvial, alluvial, lacustrine, beach, fluvial terraces deposits (Holocene)

Table 1: 128 lithotypes described in the original legend of the 1:500,000 Italian Geological Map grouped into the three categories A, B, C from EC8.

Because of the large scale of the original geologic map, the small-size Quaternary basins characterizing the Appenines are often missing. Moreover, we checked for errors associated to the 1:500,000 scale, comparing the map with very detailed geological maps (1:10,000 and 1:5,000) for the Umbria-Marche region. The comparison showed high accuracy and 60% of reliability for class A (rock), whereas highlight problems for discerning between class B and C (see report of the 2nd year activity).

References

ENV 1998-1-1, EUROCODE 8, Design Provisions for Earthquake Resistance of Structures. Seismic actions and general requirements of structures. CEN/TC 250, Draft 4, December 2001.

Servizio Geologico Nazionale. Carta Geologica d'Italia al 500,000. Servizio Geologico Nazionale editor, 1978.

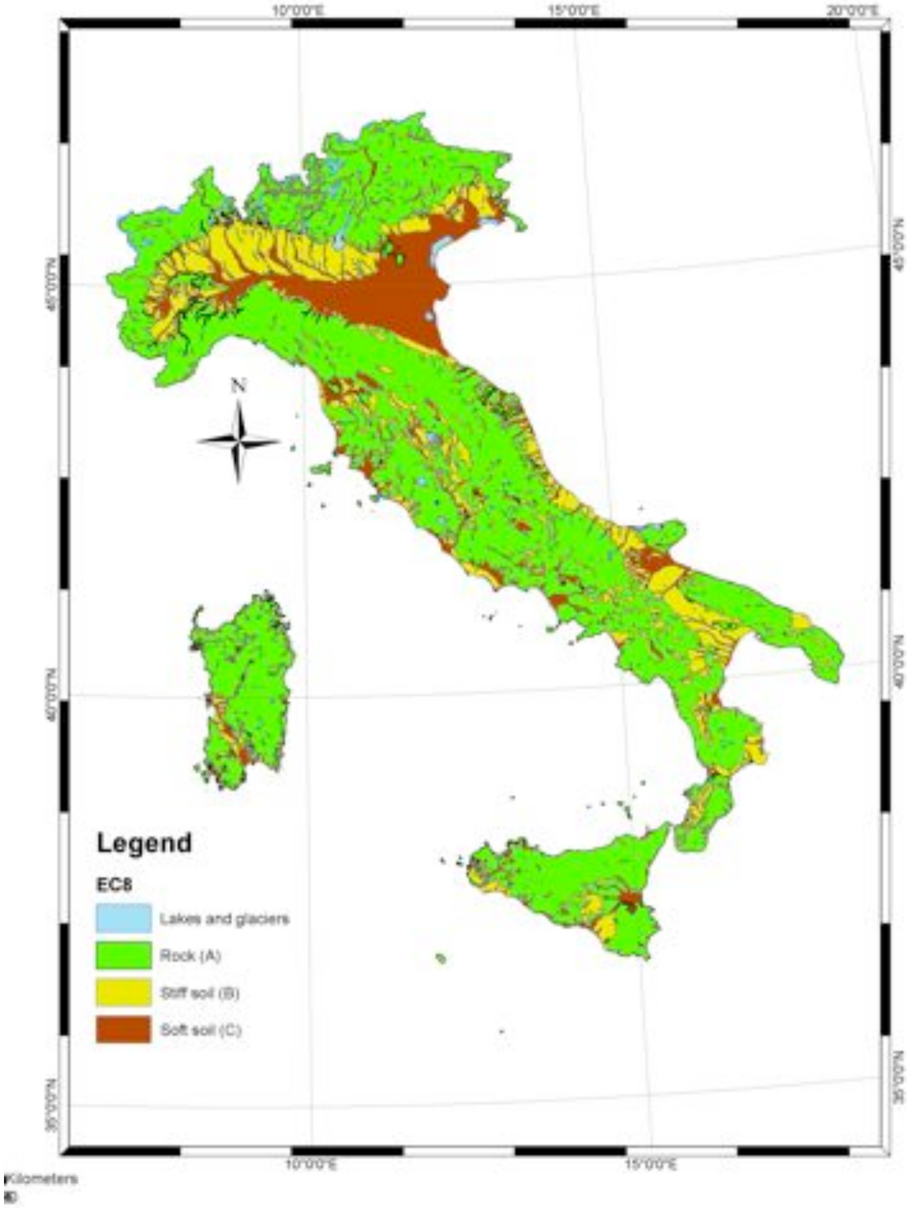

Figure 1: National geologic map at 1:500,000 scale (SGN, 1978), reclassified according to the EC8.

ANNEX 2. Correlation between Intensity anomalies and geological classification

Valerio De Rubeis, Paola Bordoni, Giovanna Cultrera, Antonio Rovelli, Patrizia Tosi

For a critical evaluation of the proposed approach, we have checked the occurrence of a systematic increment of macroseismic intensity as a function of the geological classes at a national scale.

We analyzed the Intensity field of 5 large earthquakes occurred in Italy during the XX century, as listed in Table 2.1. Only localities with intensities greater than IV MCS were taken into account.

Locality	Lat	Lon	Date	Io	# of Intensity data
Marsica, Fucino	41.98	13.62	13/01/1915	XI	879
Irpinia	41.07	15.35	23/07/1930	X	449
Irpinia	40.85	15.28	23/11/1980	X	870
Lazio-Abruzzo, Valcomino	41.67	14.05	7-11/05/1984	VIII	635
Molise	41.76	14.94	31/10/2002	VIII	704
					tot (averaged equal locations)= 2024

Table 2.1 Earthquakes of the XX century used in this study and number of data selected with I>IV MCS.

For each earthquake we computed the average isotropic pattern as a function of the logarithmic hypocentral distance R and we fit it with a polynomial function of 3rd or 4th order. We then computed the residual as difference of the Intensity to the polynomial function (Figure 2.1) and, for the municipalities where more than one earthquake was felt, we averaged the residuals of the different earthquakes. Hereinafter we refer to the average residual as "anomaly".

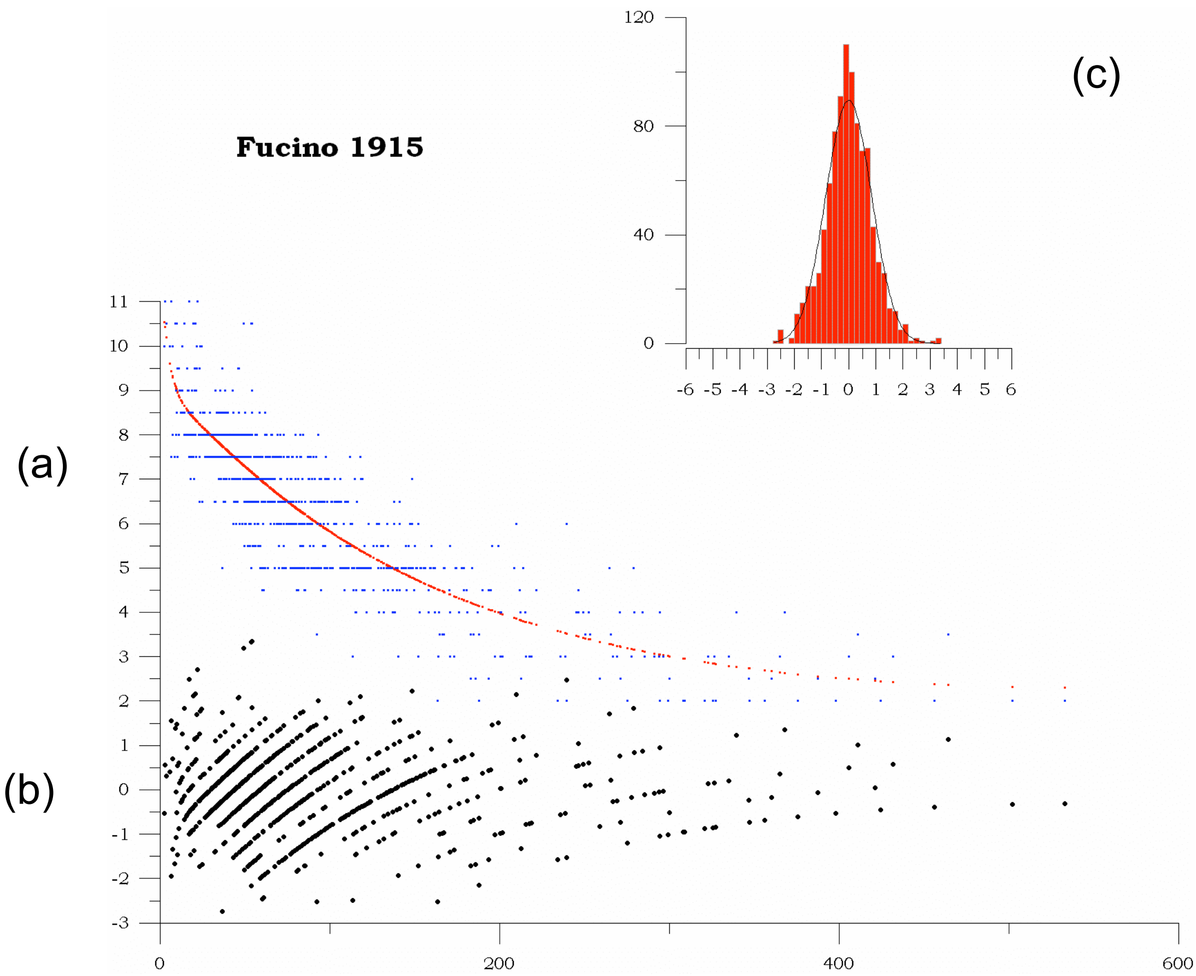

Figure 2.1: attenuation pattern of the Fucino 1915 Intensity data. (a) blu dots are the original Intensities as function of epicentral distance and red dots mark the polynomial function; (b) residual values and (c) their histogram compared with a Gaussian curve.

The comparison of the anomalies with the geological-class map does not indicate a clear correlation between softer soils and positive Intensity anomalies. That is partially related to the limitation of the Intensity datum itself, which represents an average over a wide area that can include different geological classes.
To overcome this limitation we defined a grid of 3x3 km^2 (average size of inhabited sectors) around each Intensity site. The square was subdivided into 49 cells and the anomaly value at each observation site was attributed to every cell of the grid (Figure 2.2). We then associated the Intensity anomaly of each cell to the corresponding soil class A, B or C as inferred from the Geological-Class Map.

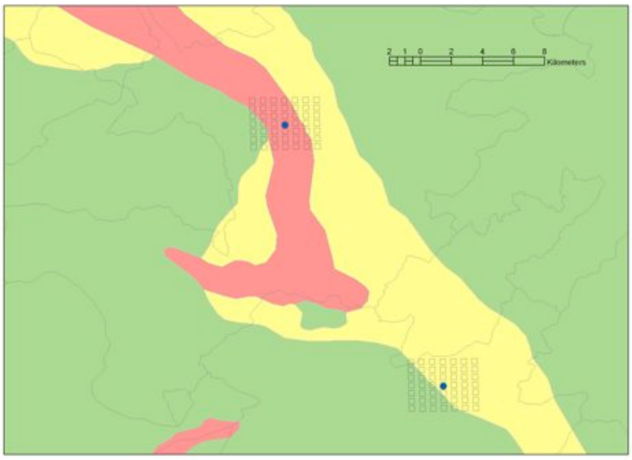

Figure 2.2: example of grid subdivided into 49 cells (squares) around each Intensity site (blue dots).

For each soil class we constructed the histogram of the anomalies (Figure 2.3) whose number of data is N_A=72614 for class A, N_B=19703 for class B and N_C=6572 for class C. Their average values are close to zero (mean(A)=0.008, mean(B)=0.121 and mean(C)=0.126), and this behavior makes difficult the correlation of the anomaly distributions with the soil classes.

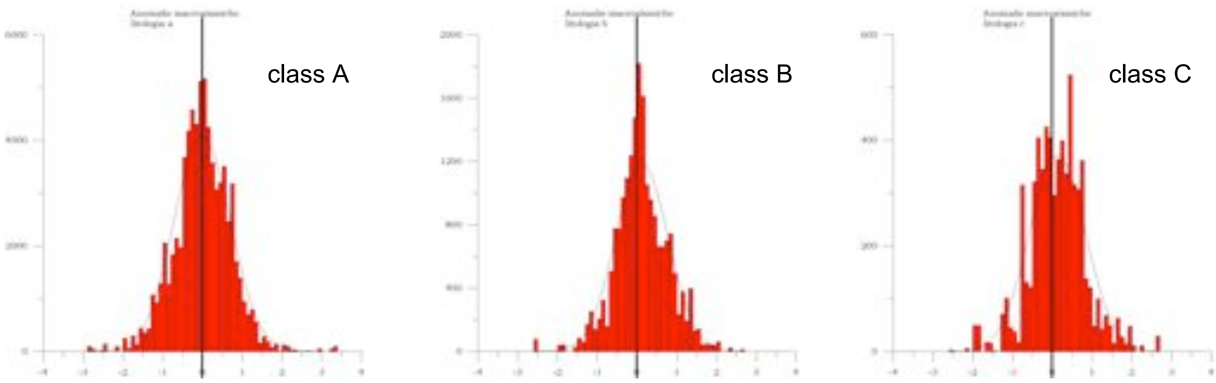

Figure 2.3: Histograms of anomalies associated to soil class A, B and C.

More sophisticated statistical approaches are then necessary to estimate the significance of possible correlation between the sign of anomaly and the soil classes, i.e. to study the asymmetry of the distribution curves.
We apply two statistical tests:
1) TEST1 gives information on the distribution asymmetry with respect to a distribution with *0* mean value
2) TEST2 investigates the size of anomalies related to the 3 soil classes.

We stress that the macroseismic data can be biased by several factors: each intensity is averaged over a large area and its estimate is not uniformly distributed over the territory; the observation can be affected by the building vulnerability; the site effects are not due to the impedance contrasts only.

Test 1

We evaluate the asymmetry of the distribution associated to each lithological class through the third-order moment *m3*, defined as:

$$m3 = \frac{1}{ns^3}\sum_{i=1}^{n} x_i^3$$

$$s = \sqrt{\frac{\sum_{i=1}^{n} x_i^2}{n-1}}$$

where n is the data number and x_i is a single anomaly value of a site class. The third-order moment enhances the departures from a zero value of anomaly, maintaining information on their sign: if *m3*=0, the distribution is symmetric, if m3<0 the negative values prevail, if m3>0 positive anomalies are more than the negative ones.
Anomaly data of Figure 2.3 give *m3*= -0.024 for class A, *m3*= 0.474 for class B and *m3*= 0.556 for class C. These results indicate that the litologies do influence the macroseismic anomalies. To ensure that these results are not due to statistical fluctuation, we compared them with the random distribution of m3 values: (1) we randomly choose from the totality of data three subsets of values whose number was equal to the real ones (Na, Nb and Nc); (2) we attribute these subsets to class A, B and C respectively; (3) we repeat this process creating 50000 representations of the same dataset and (4) we compare the distribution of m3 of these randomly chosen populations with the real results. Figure 2.4 shows that the m3 values of the real lithological subdivision are well outside the populations of the 50000 simulated ones.

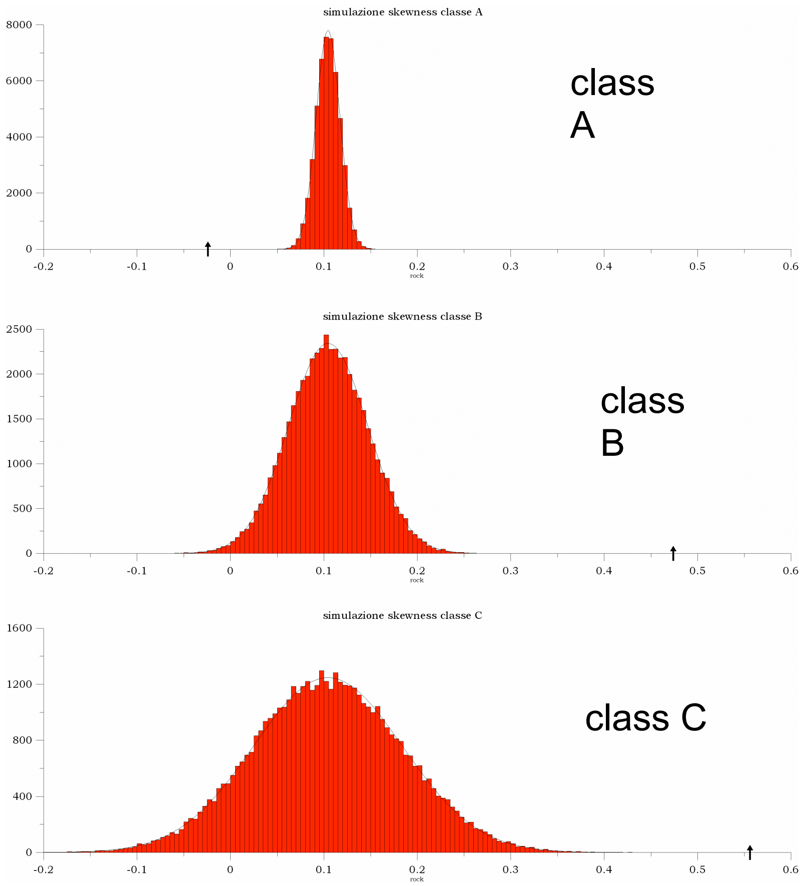

Figure 2.4: Comparison of *m3* distribution for the random population and the *m3* values of the observed dataset for class A, B and C (black arrow).

Test 2

Test 1 gave information on the distribution asymmetry in respect to *0* mean value, without any discrimination of the size of specific intensity anomaly groups. Therefore we investigate further in detail the role of the anomaly size. From intensity residual data, five bins are constructed as:

bin	type	res MIN	res MAX
1	large attenuation	<	-1.0
2	small attenuation	-1.0	-0.5
3	neutral behavior	-0.5	0.5
4	small amplification	0.5	1.0
5	large amplification	1.0	>

Each lithological subdivision has consequently a five-value distribution. For example, if lithology A represents a tendency to attenuate, it should have one or both attenuation classes with more elements than an uncorrelated distribution.

To ensure statistical significance of the deviations, the five distributions of each lithological class are computed for 50000 randomly chosen representations of the

same dataset (see Test 1). Each of the five behavior bins gives, from the simulation, a distribution of random fluctuations. Real case values are normalized to such distributions and compared in Figure 2.5:
Lithology A (hard rocks) has both attenuation classes much more numerous than simulation (several σ orders) whereas neutral and highest amplification are under represented;
Lithology B has the two attenuation classes with less elements than simulations, while neutral and highest amplification are significantly more numerous;
Lithology C behaves for attenuation as Lithology B, and it has both amplification classes more numerous than random simulation.
The results of this test are in agreement with results of Test 1, giving a detailed insight of peculiar intensity site response in terms of attenuation, neutral and amplification classes.

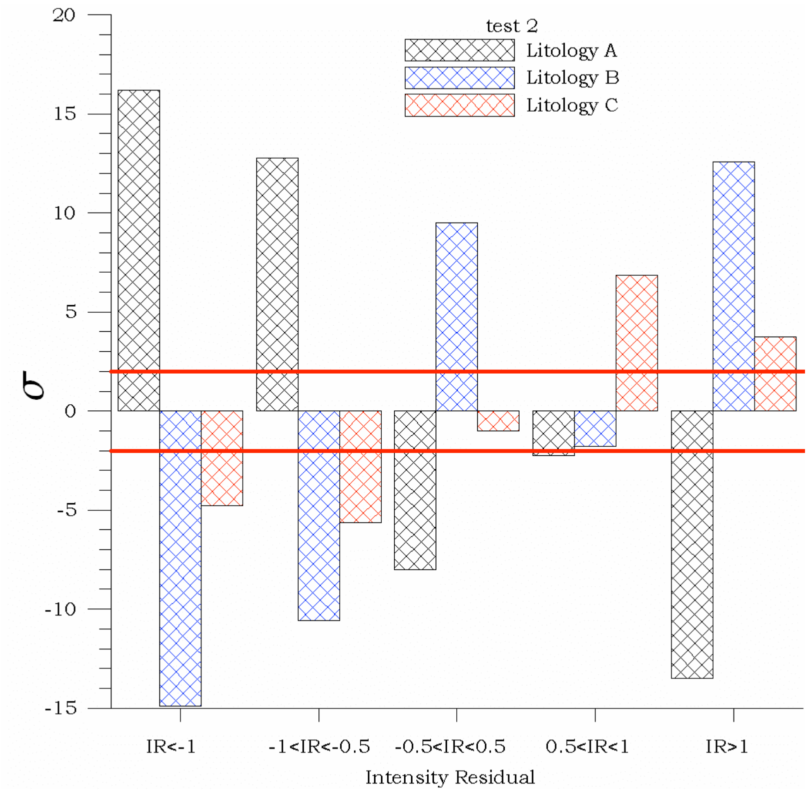

Figure 2.5: Detailed characterization of amplification/attenuation classes for the three lithologies in respect to a randomly chosen simulated representation. In abscissa each lithology is subdivided into five intensity residual classes, in ordinate the number of elements of each class for the three litologies is normalized in standard deviations units σ, as resulted by 50000 randomly chosen representations; lines are drown to highlight statistically significant departures.

ANNEX 3. Correction factors derived from EC8 5/2001 elastic response spectra

Lucia Luzi, Giovanna Cultrera, Paola Bordoni, Antonio Rovelli

We assume that the effect of local geology on hazard parameters (PGA, PSA, Housner intensity, amplification factor Fa) is described by the site dependence of elastic response spectra PSA prescribed by EC8 (ENV, 1998):

PSA(T) -5% damping-	**T**	where:
a_g S [1 + 1.5 T/Tb]	[0, Tb]	a_g= design ground acceleration (PGA with return period 475 years) referred to bedrock;
a_g S 2.5	[Tb, Tc]	S = soil parameter;
a_g S 2.5 [Tc/T]	[Tc, Td]	Tb, Tc, Td = corner periods.
a_g S 2.5 [Tc Td / T^2]	[Td, 4sec]	

PSA is controlled by the four parameters S, Tb, Tc, Td that depend on the soil classes and earthquake magnitude. In this study we have adopted the values proposed for M>5.5 (Type1 spectrum; Figure 3.1).

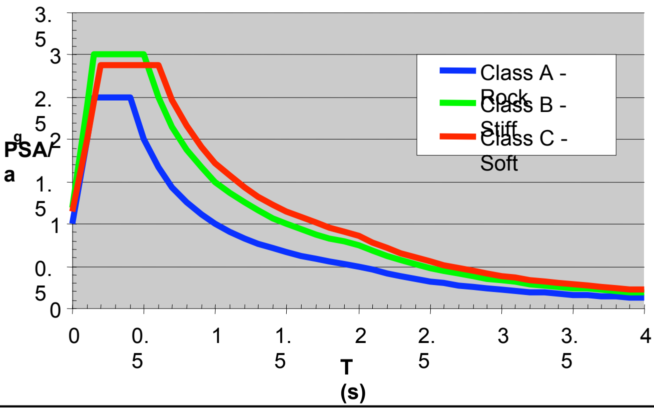

Soil Type	**Vs (m/s)**	**S**	**Tb (s)**	**Tc (s)**	**Td (s)**
A	> 800	1.0	0.15	0.4	2.0
B	400-800	1.2	0.15	0.5	2.0
C	< 400	1.15	0.20	0.6	2.0

Figure 3.1: Shapes and parameters for elastic response spectra (pseudoacceleration with 5% damping) of Type 1 earthquakes (M>5.5), according to soil types (EC8 Draft 12/2001).

We represent the variability due to the soil classification of the GCM map through the correction factors (Figure 3.2; Table 3.1), i.e. the ratio of the hazard parameters to the ones computed for class A (S=1). Figure 3.3 to 3.5 show the final hazard maps taking into account the correction factors (see report of the 2^{nd} year activity).

class	**cf_PGA**	**cf_PSA (0.3s)**	**cf_PSA (1s)**	**cf_PSA (2s)**	**Fa**
A-rock	1.0	1.0	1.0	1.0	1.0
B-stiff	1.2	1.2	1.5	1.5	1.47
C-soft	1.15	1.15	1.725	1.725	1.65

Table 3.1: Correction factors (cf) for PGA, PSA at fixed periods, 0.3s, 1.0s and 2.0s, and amplification factor Fa.

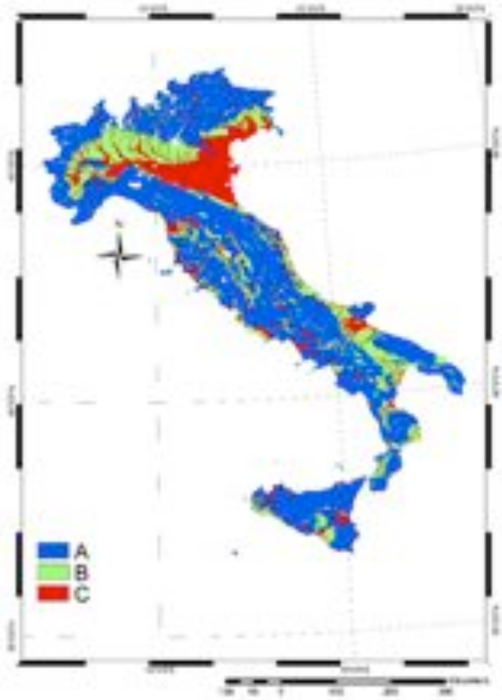

Figure 3.2: Map of correction factors for soil class A, B and C.

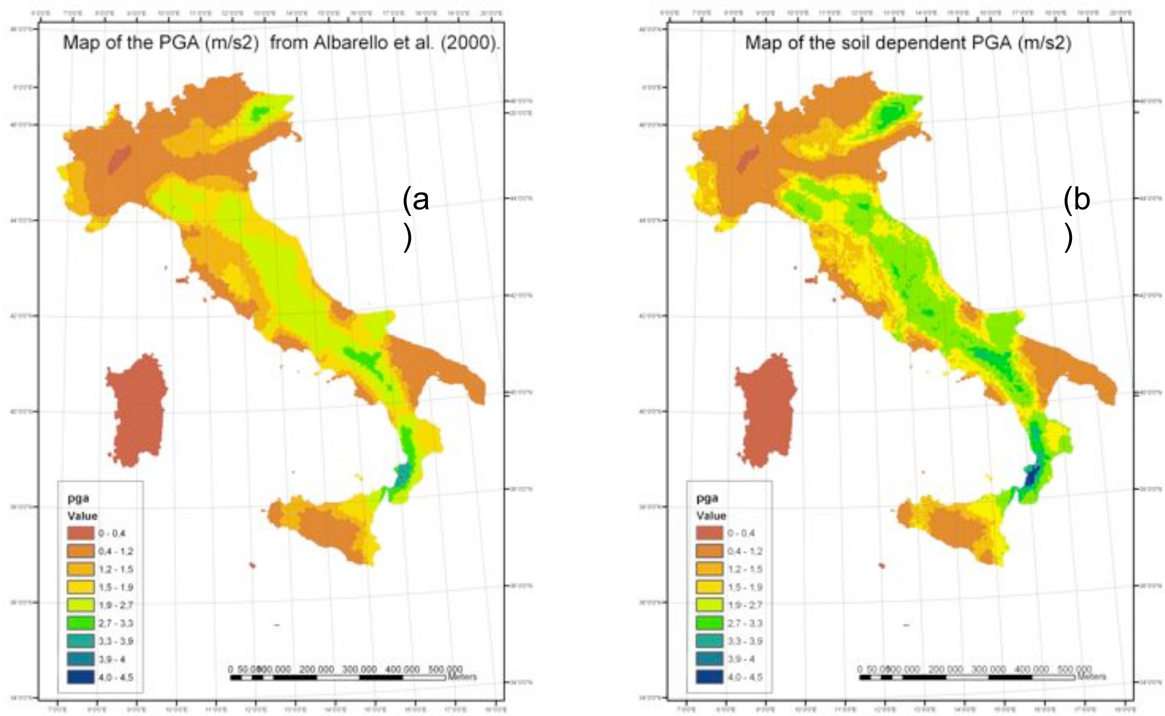

Figure 3.3: (a) Map of the PGA (m/s2) at 10% probability of occurrence in 50 years (return period = 475 years), from Albarello et al. (2000); (b) map of the site-dependent PGA, obtained by correcting the map in (a) with the PGA correction factors.

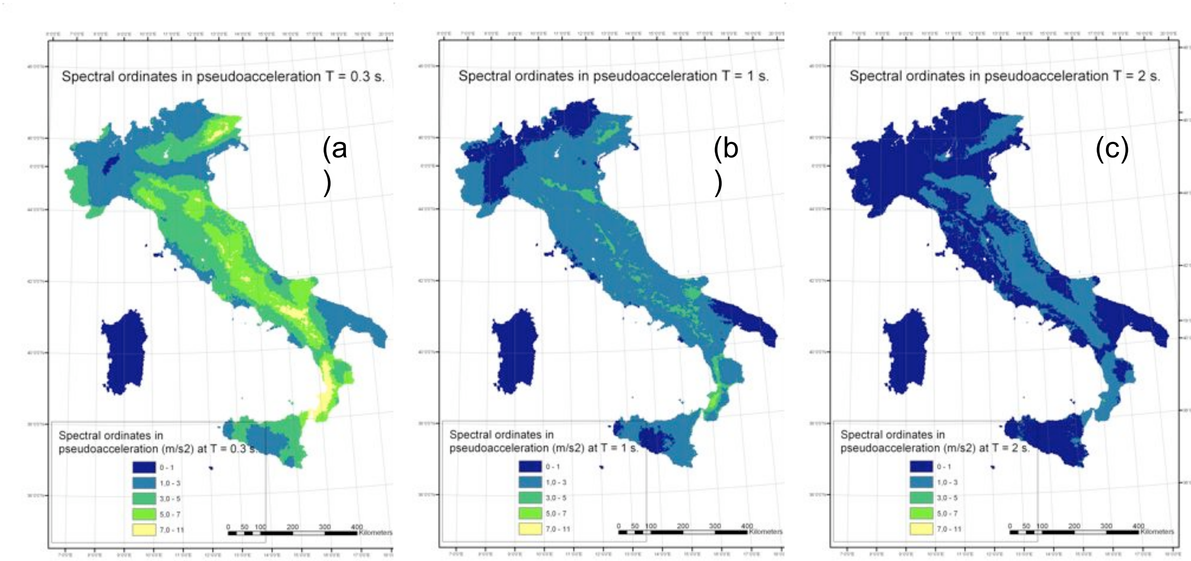

Figure 3.4: Maps of site–dependent PSA (m/s^2) at (a) T=0.3s, (b) T=1.0s and (c) T=2.0s, using a reference PGA hazard map of Albarello et al., 2000 (see Figure 3.3).

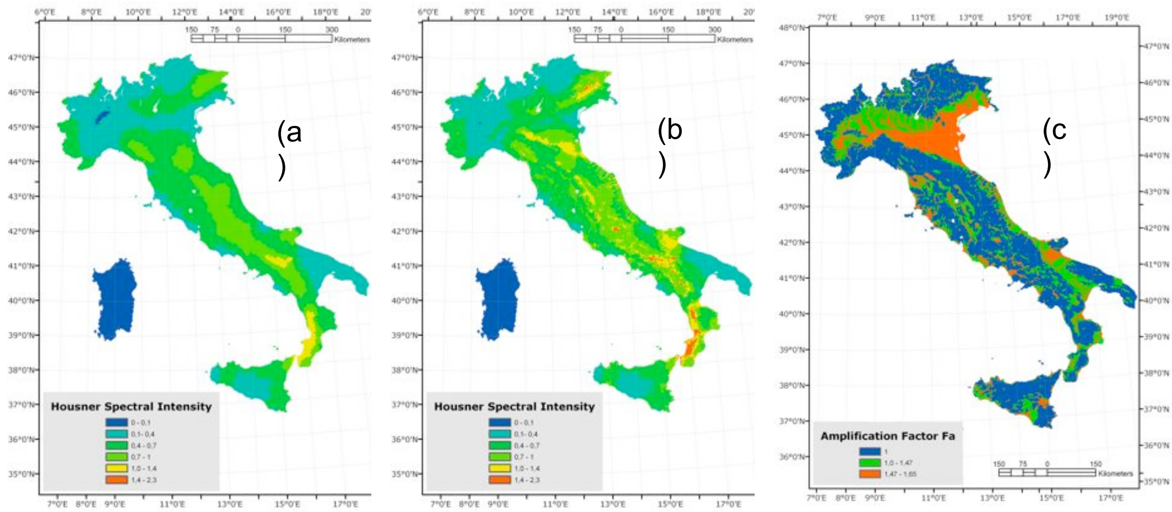

Figure 3.5: Maps of (a) Housner (1952) Intensity (m), (b) site–dependent Housner Intensity (m), and (c) amplification factor Fa (Pergalani et al., 2002), using a reference PGA hazard map of Albarello et al., 2000 (see Figure 3.3).

References

ENV 1998-1-1, EUROCODE 8, Design Provisions for Earthquake Resistance of Structures. Seismic actions and general requirements of structures. CEN/TC 250, Draft 4, December 2001.

Housner GW (1952). Spectrum intensities of strong motion earthquakes. Proceeding of the Symposium on Earthquakes and Blast Effects on Structures. Earth. Eng. Res. Inst., Kohavi R. and Provost F (1998). Glossary. *ML Journal*, page 272, 1998.
Pergalani F., M. Compagnoni, and V. Petrini (2002): Valutazione degli effetti di sito tramite analisi numeriche e sperimentali nell'abitato di Città di Castello: analisi, confronti e utilizzo dei risultati. Ingegneria Sismica, 1, 66-77 (in Italian with English abstract).

ANNEX 4. Variations of probabilistic hazard parameters inferred from 2D numerical modeling at local scale, the Città di Castello case study

Giovanna Cultrera, Paola Bordoni, Simone Marzorati

A further test has been performed to compare the correction factors of Table 3.1 to those deriving from a numerical simulation of the Città di Castello (Central Italy) basin where many geological and seismological data were available.

Model of the basin

We define a 2D profile of the basin of Città di Castello following Bordoni et al (2003). The profile crosses the town and the sites where weak motion and noise measurements were performed (Figure 4.1), from station CD20 to CD05.

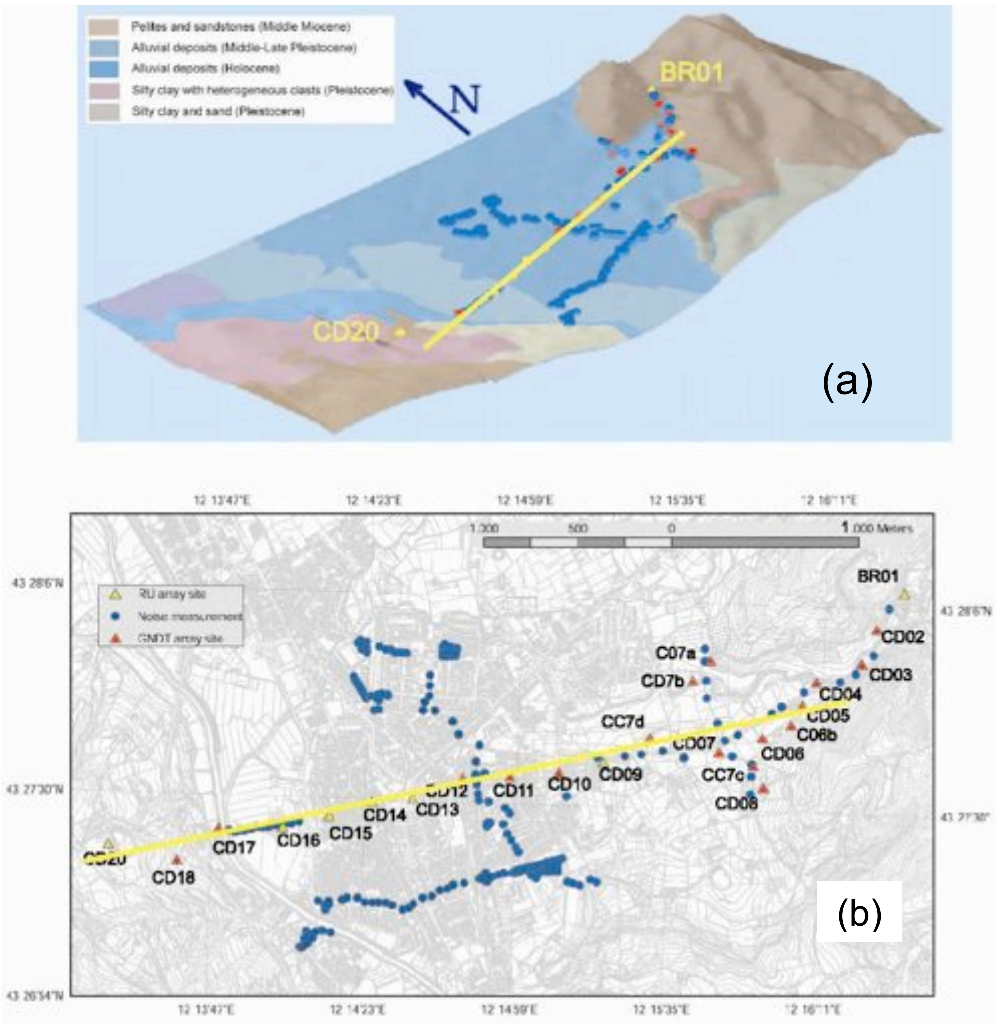

Figure 4.1: (a) topography and geology of the study area; (b) station locations (triangles) and noise measurements sites (dots). The yellow line is the trace of the topographic profile in Figure 4.2.

The geological setting, the geometry and the velocity model are defined after Bordoni et al. (2003) and Crespellani et al. 2003 (Table 4.1 and Figure 4.2).

Table 4.1: Velocity model used for the 2D simulation

	bedrock	(1) Lacustrine Pleistocine deposits	(2)Alluvial Pleistocene deposits	(3) Alluvial Holocene deposits
Vs (m/s)	1100	370	250	200
Rho (g/cm3)	2.2	2.1	2.1	1.9
Q	100	20	20	15
1/Q		0.05	0.05	0.07

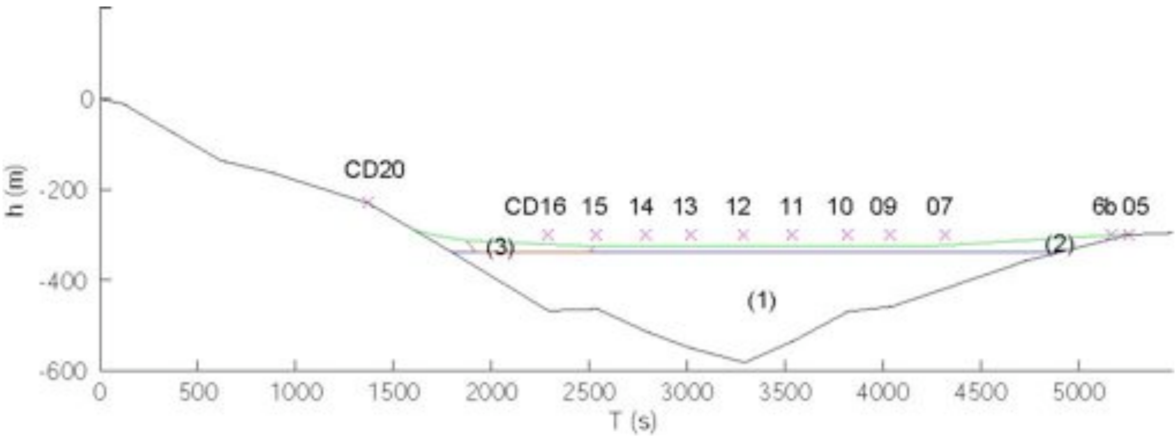

Figure 4.2: 2D profile (yellow line in Figure 4.1) with the recording seismic stations, as used for the simulation. Refers to Table 4.1 for the seismic parameters of soil (1), (2) and (3).

2D modeling

We simulate the SH-wave response of the 2D basin of Figure 4.2 using the finite-difference code (Caserta, 1998; Caserta et al., 2002). The computation was performed through a Web Interface for Seismological Applications (WISA; Caserta et al., 2004), a Web tool that helps the user in making 2D numerical simulations of the interaction between a vertically incident seismic radiation and near-surface geological structures. The modeling was performed through parallel multiprocessor machines, getting synthetics time histories of the displacement at the free surface.

We use a delta-like function (Gabor function) as SH plane wave input. The duration of synthetics was 10 seconds with a maximum frequency of 8.0 Hz, and spatial steps of 10 meters (Figure 4.3).

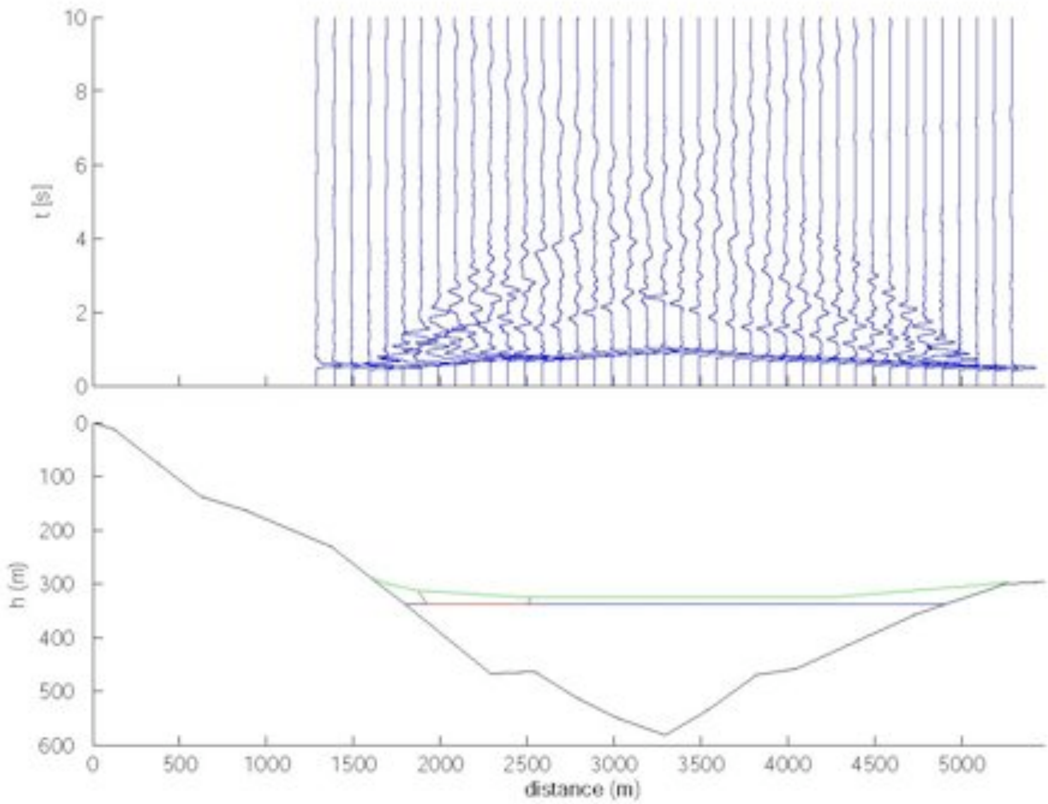

Figure 4.3: Synthetics time series along the profile.

The 2D synthetic transfer functions are compared with (1) 1D computations at the array sites (Haskell-Thomson technique) and (2) earthquake and noise recorded data:

(1) The 2D simulations are similar to the 1D results (Figure 4.4). The ratio of horizontal-to-vertical dimensions of the profile is about 10, such that the energy diffracted from the edges is attenuated very fast due to the low Q of the soft layers.

(2) The comparison between 2D simulation and weak-motion spectral ratios and the noise H/V ratios is shown in Figure 4.5. In general, the fit of the simulation with the H/V noise peaks is very good. Note that the fundamental resonance peak from the noise analysis at the central stations are below 1Hz, where the signal-to-noise ratio of the earthquake do not allow to use the empirical transfer functions (ETF). In the intermediate frequency range, where the ETFs have a large amplification, the simulation are not able to reproduce the local response because of the lack of information on the details of the geological structure (we match the mean value of velocity but we cannot take into account of its fine structure).

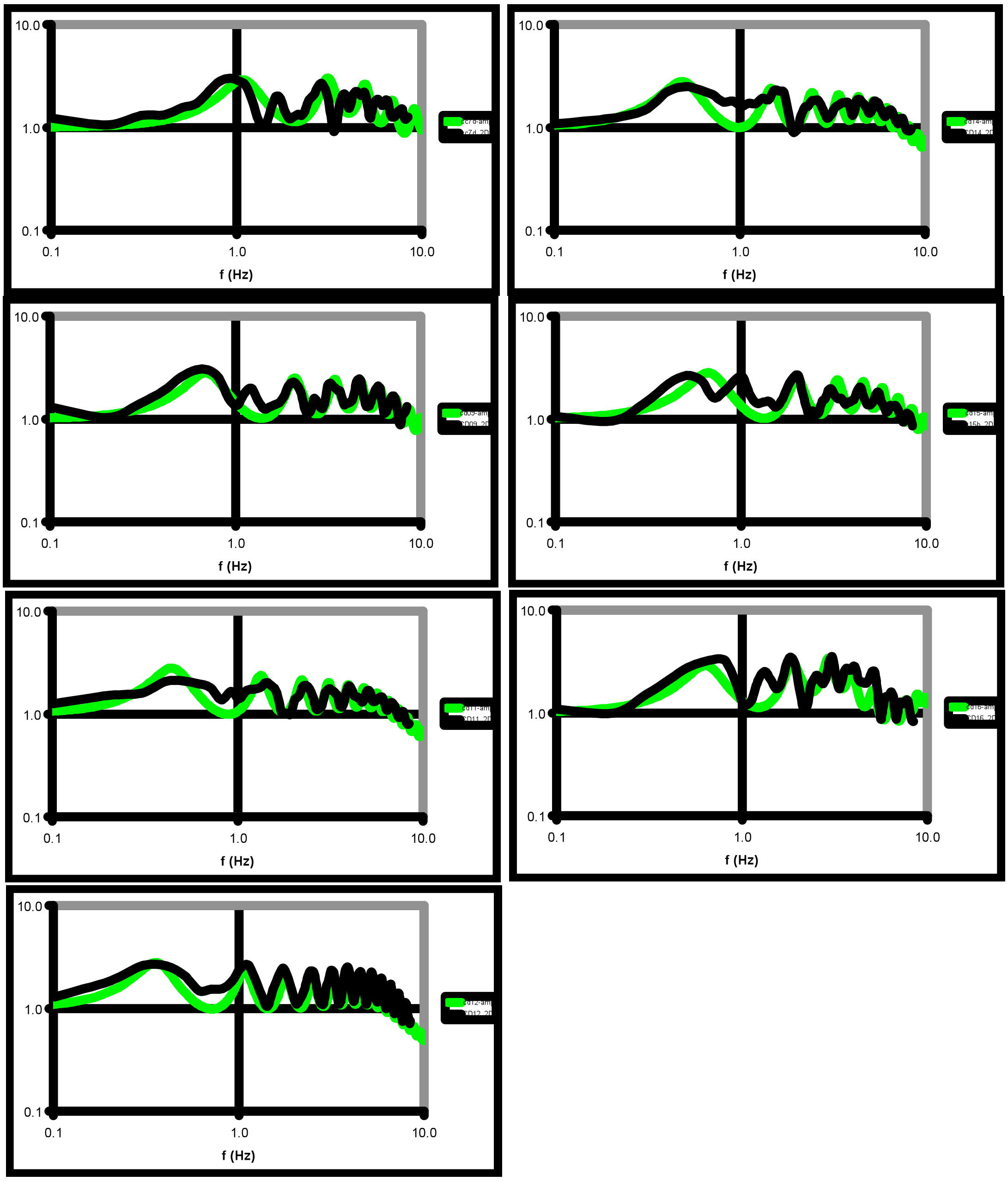

Figure 4.4: comparison between 1D (green line) and 2D (black line) transfer functions.

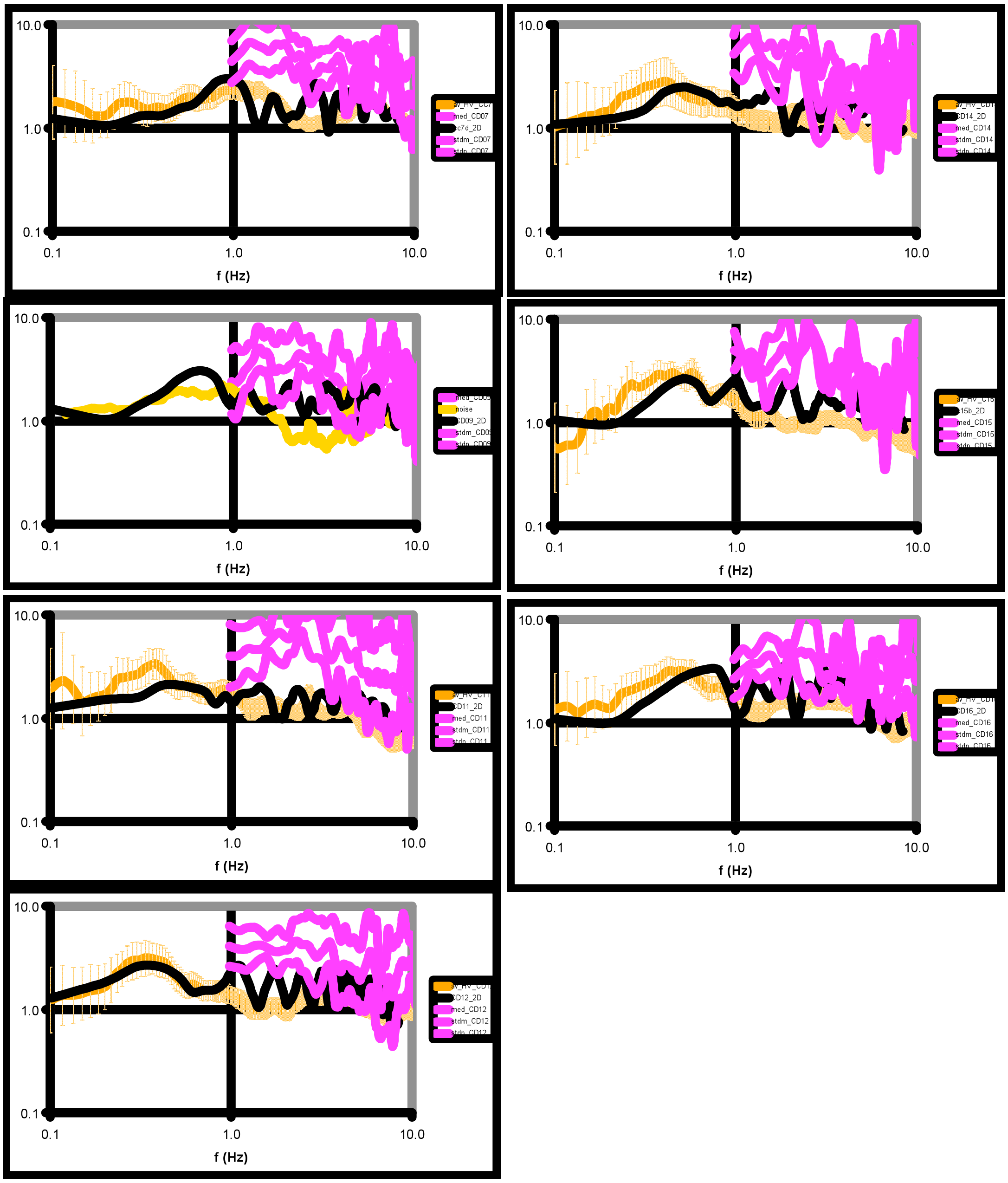

Figure 4.5: comparison between 2D transfer function (black line), weak-motion spectral ratios (pink line) and the noise H/V ratios (orange line).

Elastic response spectra

We use the simulated transfer functions to evaluate the variation of response spectrum values inside the basin, as follow:

1) generation of synthetic accelerograms to be used as bedrock input;
2) convolution with the 2D synthetic transfer functions;
3) computation of the elastic response spectra (PSA, PSV) and other strong motion parameters (PGA and Housner Intensity) and their ratio to the same quantity using the bedrock input motion.

First of all, we generated bedrock synthetic accelerograms (code Belfagor 1.02, Mucciarelli et al., 2004; Figure 4.6) using the initial condition of Sabetta and Pugliese (1996) spectrum for a M=5.8 earthquake at R=20 km. The elastic response spectrum of the simulated accelerograms mimics the EC8 spectral shape for bedrock sites and Type 1 earthquakes (Ms>5.5), anchored to the PGA value prescribed by the national hazard map for Città di Castello (Class II, i.e. expected PGA of 0.25 g with 10% probability of occurrence in 50 years).
We then convolved the bedrock synthetic accelerogram with the 2D synthetic transfer functions (Figure 4.7) and we computed the elastic response spectra and at each site (PSA, PSV) and their ratio to the input motion (Figure 4.8).

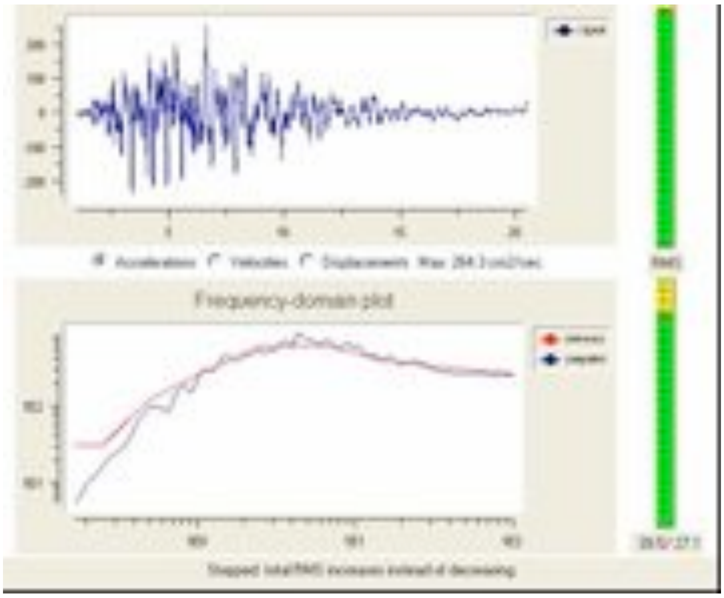

Figure 4.6: synthetic acceleration time series (cm/s^2) and response spectrum (blue line) for a bedrock site. Red line is the reference elastic response spectrum with 5% viscous damping, for Type 1 earthquakes (Ms>5.5), anchored to PGA=0.25g.

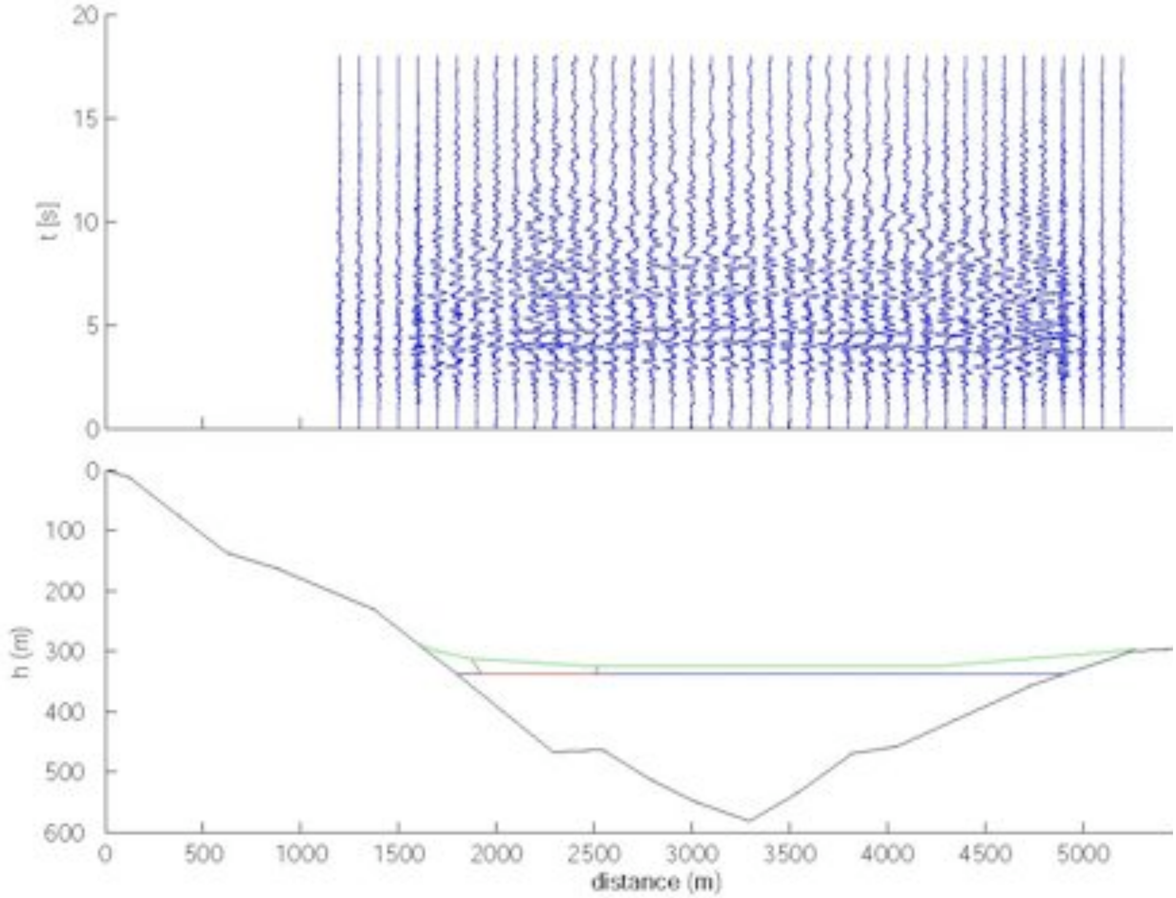

Figure 4.7: 2D synthetics time series of Figure 4.3 convolved with the bedrock synthetic acceleration of Figure 4.6.

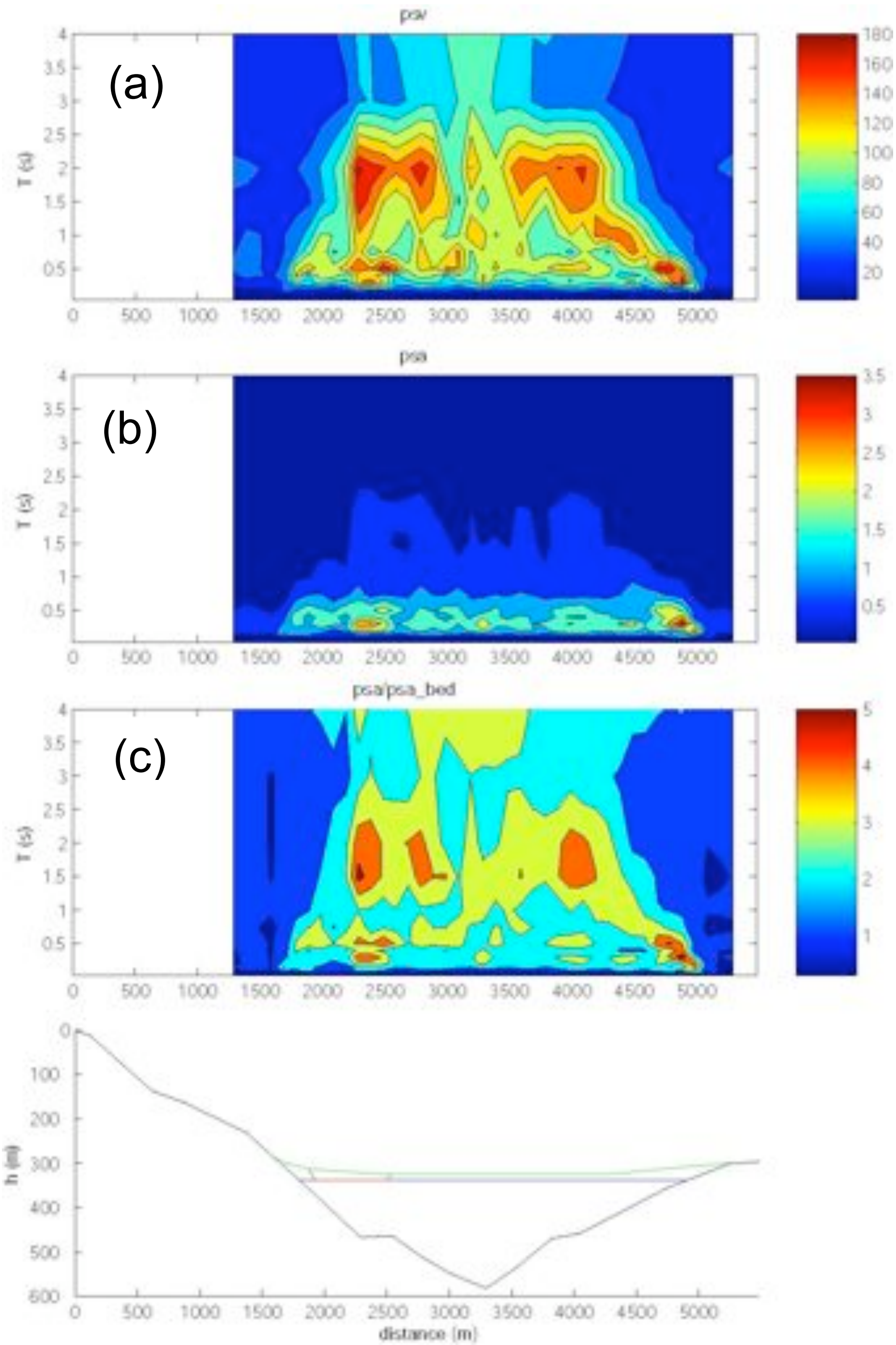

Figure 4.8: Contour plot of (a) PSV, (b) PSA and (c) PSA ratio.

The mean increment of the hazard parameters along the profile is compared with that expected for the outcrop soils of class B and C as inferred from the Geological-Class Map of the same area (Figure 4.9). The computed Fa (Housner Intensity variation) and PGA variation is greater than values listed in Table 1 by a factor 1 to 2. The small difference is probably due to the fact that the EC8 values come from an average over many different geological settings and geometries whereas this simulation reflects a specific velocity structure.

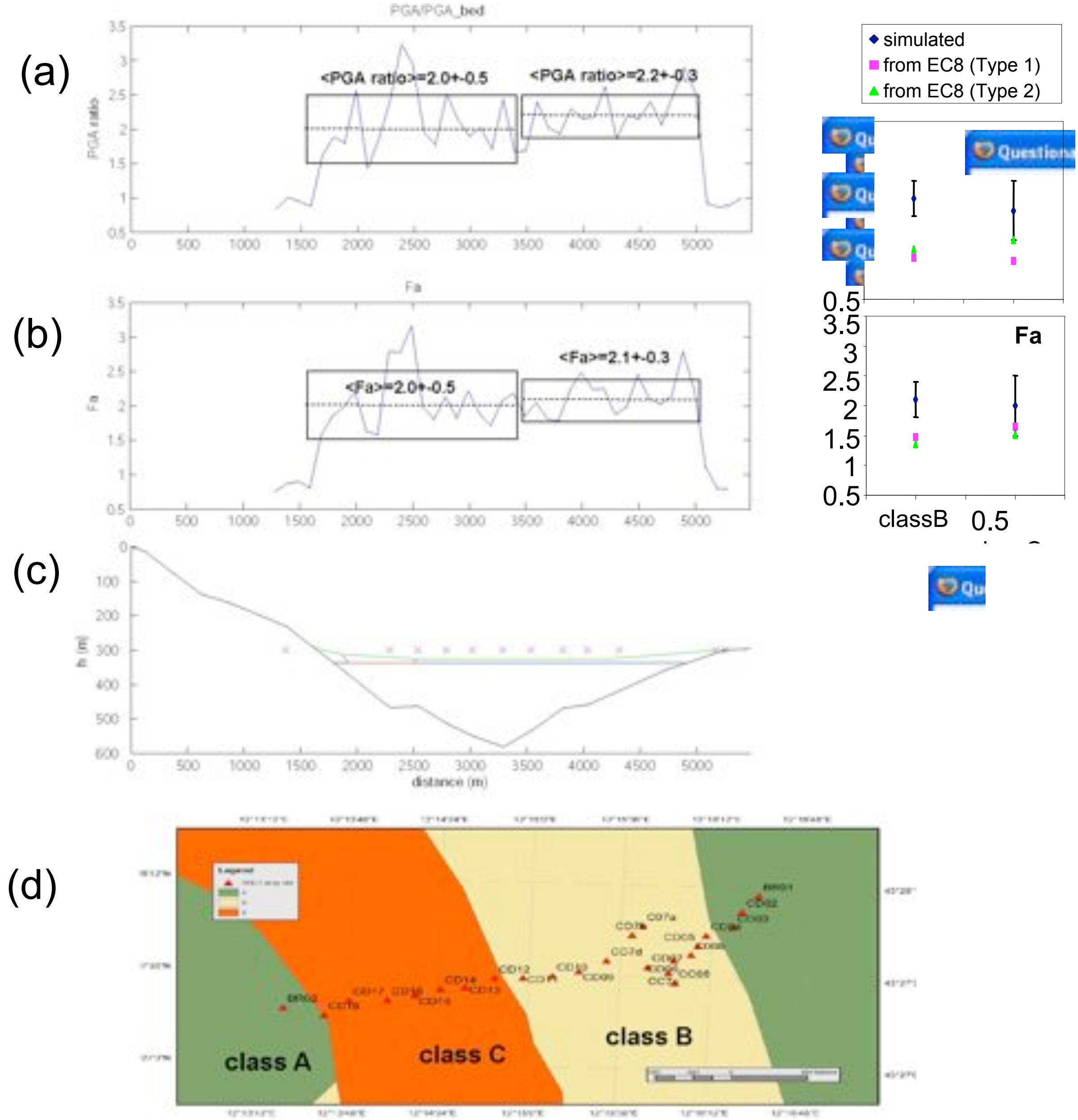

Figure 4.9: (a) PGA ratio and (b) Fa along the profile (c) from the simulation of Figure 4.7. The boxes refer their average +-1 standard deviation in the areas of class B and C as inferred from the zoom of the Geological-Class Map around Città di Castello (d). They are compared with the computed correction factors cf_B and cf_C (e).

References

Bordoni P., G. Cultrera, L. Margheriti, P. Augliera, G. Caielli, M. Cattaneo, R. de Franco, A. Michelini, and D. Spallarossa (2003). A microseismic study in a low seismicity area: the 2001 site-response experiment in the Città di Castello basin (Italy). Annals of Geophysics, VOL. 46, N. 6, December 2003.

Caserta, A., 1998. A time domain finite-difference technique for oblique incidence of antiplane waves in heterogeneous dissipative media. Annali di Geofisica 41, 617-631.

Caserta, A., Ruggiero V., Lanucara P., 2002. Numerical Modelling of dynamical interaction between seismic radiation and near-surface geological structures: a parallel approach.Computer & Geosciences, 28/9, 1071-1079.

Caserta A., Giuffrida C., Ruggiero V., Lanucara P., Firmani B. 2004. Input Data Web Interface for Numerical Simulations of Seismic Wave Propagation. ESC XXIX General Assembly Abstract Books, pp. 85.

Crespellani T., C. Madiai, and G. Simoni (2002). Indagini geotecniche per la valutazione degli effetti di sito in alcuni centri dell'Alta Valtiberina, Ingegneria Sismica, 1, 15-32 (in Italian with English abstract).

Sabetta F. and A. Pugliese (1996). Estimation of response spectra and simulation of nonstationary earthquake ground motions. Bulletin of Seismological Society of America, 86-2, 337-352.

Mucciarelli M., Spinelli A. and F. Pacor (2004). Un programma per la generazione di accelerogrammi sintetici "fisici" adeguati alla nuova normativa. Proceedings of XI National Congress of Italian National Association of Earthquake Engineering, ANIDIS, "L'ingegneria sismica in Italia", Genova 25-29 January 2004.

Servizio Geologico Nazionale. Carta Geologica d'Italia al 500,000. Servizio Geologico Nazionale editor, 1978.

ANNEX 5. Database of the national scale enquiry about surface geology

Paola Bordoni, Diego Sorrentino, Fawzi Doumaz, Fabrizio Marra, Giovanna Cultrera, Lucia Margheriti, Antonio Rovelli

Questionnaire Description

Within the project we launched a national-scale enquiry whose main goal was the estimation of the buildings distribution on the three soil classes corresponding to those of the CGM. In addition, the enquiry allows us to collect availability of geographic and geotechnical data.

To collect the data we mailed a questionnaire to the 8101 Italian Municipalities. A web-based form was also available at the website www.ingv.it/effettisito to give the Municipalities the possibility to answer the enquiry by internet (Figure 5.1). Fourteen months after sending, we received 1953 answers of which 1424 were by mail and 529 by internet. They represent the 24% of the 8101 contacted. Figure 5.2 shows for each of the 20 Italian Regions the percentage distribution of answers scaled to the total municipalities of the Region. Note that high risk 'Regions' like Campania and Calabria do not have a high answer percentage.

We organized the received forms in a dedicated database (see product 3) on a Microsoft Access platform. The database is the result of the union of two different databases: one obtained through the optical reading of the paper forms and one through a web-based form. Because we developed quite a complex form, many optical engines were involved in reading it hence the reading was performed by a professional company. They produced an image database interrogatable by name and ISTAT code for the Pegasus platform as well as an Access database with relationships following the structure set up for the Linux MySQL online version.

Because we were aware that only a small proportion of the Municipalities employ specialized technicians, we made an effort to simplify the description. In addition the form had some fields devoted to the description of the compiler's expertise (geologist, engineer, architect, others). We asked the Municipality technicians to fill in the form using the available geological and geotechnical data without making any ad-hoc investigation.

The core of the questionnaire is in the first 3 questions (see Figure 5.1), where they have to only take into account the territory of the Municipality with housing, to subdivide it into three categories according to the geological description in Table 1 and to compute the percentage of housing built over them. To underline the first order request of the enquiry, we set seven percentage categories and they were asked to put the computed percentage in one of them.

Rock	volcanic rock, intrusive rock, metamorphic rock, sedimentary rock (*limestone, "dolomie", sandstone, shale, conglomerate*)
Stiff soil	cohesive overconsolidated deposit (*clay and silt*); granular cohesionless dense deposit (*sand, gravel, slightly cemented sandstone; piroclastic deposit like 'pozzolane', 'lapilli', ashes*)
Soft Soil For thickness less than 3 metres, the underlying deposit must be taken into account	cohesive consolidated or underconsolidated deposit; granular cohesionless loose deposit (*sand, gravel*) like those infilling river valley, alluvial plain, coastal plain, intramountain basin; alluvial-lacustrine-marsh deposit; loose slope deposit

Table 1: description set for the questionnaire which was used as the basis for the percentage computation.

Figures 5.3 to 5.5 show the first 3 questions translated into English and histograms of the answers. The histograms show the frequency distribution of answers over the seven percentage categories plus 'double answer' and 'no answer' categories. Note that a 5% of 'no answer' for the first question increases to a 24% in the second question.
In the first question (Figure 5.3) we asked them to compute the percentage of housing built over both "Rock" and "Stiff Soil" geological categories together and the geological category "Soft Soil". In the second question (Figure 5.4) we asked them to compute from the percentage obtained of the "Rock + Stiff Soil" category, the percentage of housing built respectively on the "Rock" and "Stiff Soil". Next we asked them to compute from the percentage obtained of the "Soft Soil" category the percentage of housing built over two sediment thickness categories (Figure 5.5).

Results and Discussion: Comparison between the Database and the Geological Class Map (GCM)

The national scale enquiry was driven by the idea to put the result straightway in the hazard maps. The 24% of answers we received are distributed evenly along the country (Fig. 5.2) which is quite a good result. However, such percentage is not high enough to justify their use in the hazard map. Investigation of their effect in hazard map will be the object of future study.
In the present report we performed a preliminary elaboration of the collected data and we investigated the differences with the GCM information.

First of all, we assume that the answers contained in the database are true as shown by the feasibility study of the project done before sending the 8101 questionnaires. In that study we selected a sample of 10 Municipalities distributed along the national territory and checked their answers using 1:100,000 geological maps and 1:25,000 topographical maps (edited respectively by Servizio Geologico Nazionale and Istituto Geografico Militare). The agreement between them is also the result of the very wide range of percentage categories we set.
We then computed the percentage of territory with buildings on each geological class using the database, and the percentage distribution of the 3 geological classes inside the Municipality boundary following the GCM. The latter step was easily performed using GIS software (ARCGIS 8.3). Note that for the GCM case we are not referring this percentage to the housing but we are instead considering all the municipality territory. 43% of analyzed municipalities has more than 60% of urbanized territory on class C and the analysis of the GCM does not show the same percentage of soil classes; in particular, the soft soil is less represented. This should not be merely interpreted as a lack of detail of the GCM, rather as due to buildings concentrated on the smaller soft part of the territory. We cannot exclude, moreover, that municipalities reported buildings on manmade infillings not shown in the GCM.

We chose eight Municipalities as typical examples of several characteristically geographical and geological settings in Italy (Figure 5.6) and in Figure 5.7 are shown the pie charts of the percentages computed. The Municipalities of Melito, Corato and Ampezzo allow us to highlight differences and the complementary of information:

- Melito is totally on rock for the GCM while the Municipality reports only 1% of housing on rock and a dominant percentage on thin soft soil. A lack of detail of the GCM is part of the explanation of such difference, which is the easiest problem one can reckon working on such a subject and also the easiest to cope with because much detailed geological maps are available.
- Corato and Ampezzo are predominantly on rock for the GCM with about 10% of stiff and soft soil, while their Municipalities report predominantly soft and stiff soil. In this interesting case the difference can be explained by the urban development over the soft and stiff soil. This is a more difficult task to tackle at a national scale as the digitalization of the urban setting is not at all advanced.

On such basis, we conclude that the questionnaire is a good data gathering tool for pointing out area where more detailed microzonation investigation must be performed. The questionnaire can also be a powerful tool to increase awareness of Municipality Administration and the lack of involvement could be overcome by coordination at the Region levels.

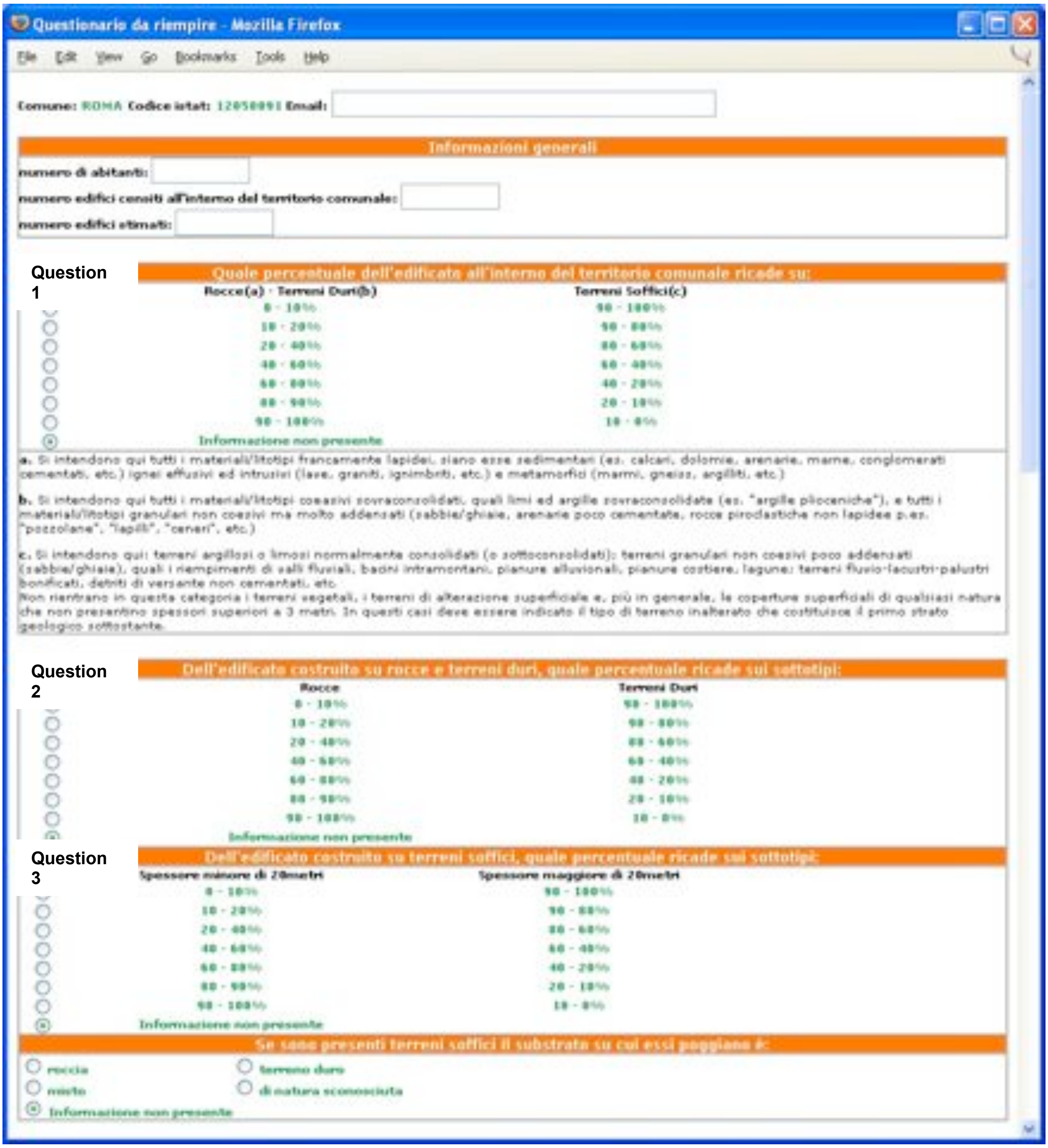

Figure 5.1: Questionnaire available at the website www.ingv.it/effettisito. Refer to the Table 1 for translation of Question 1-3

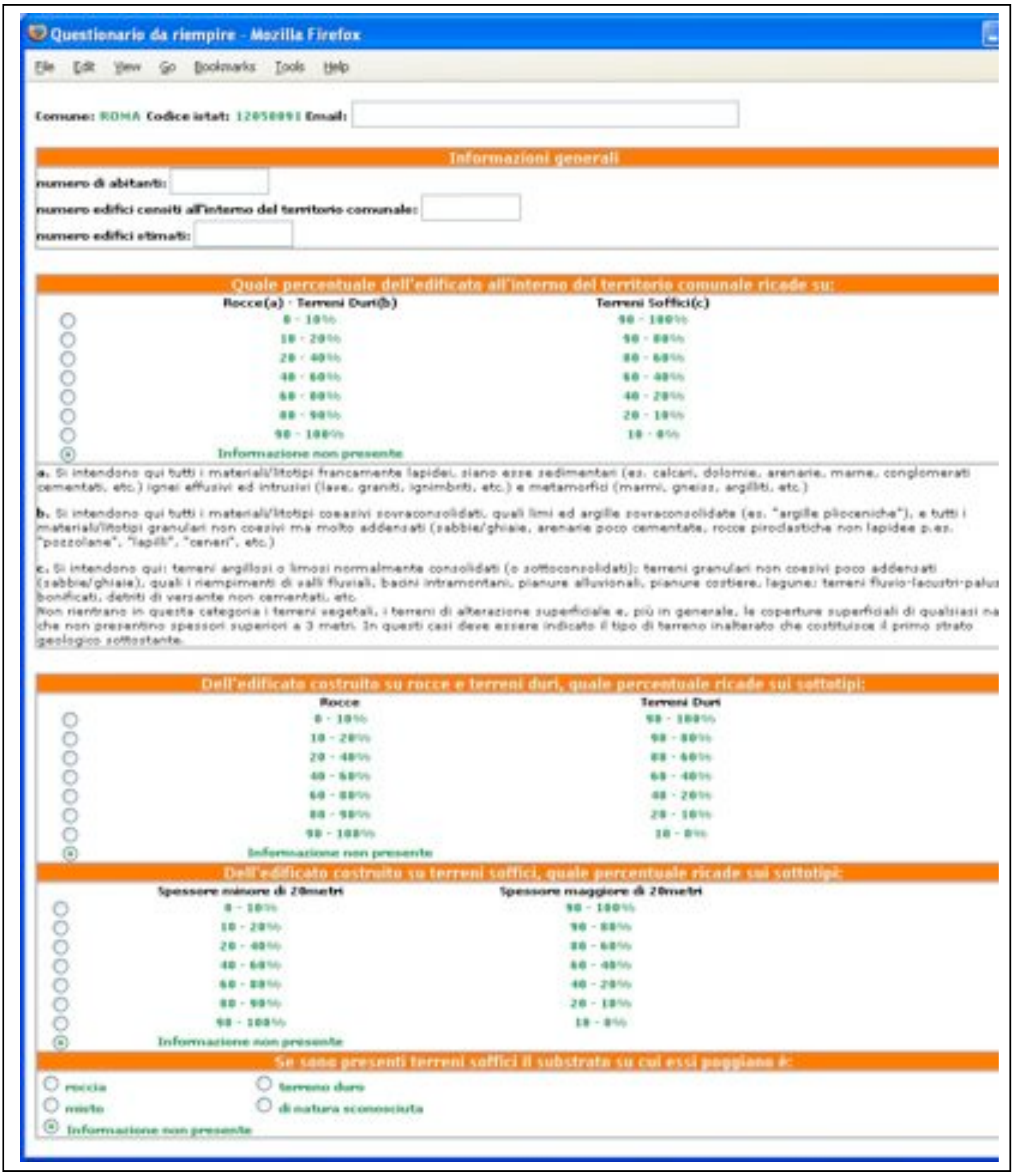

Figure 5.1: continue

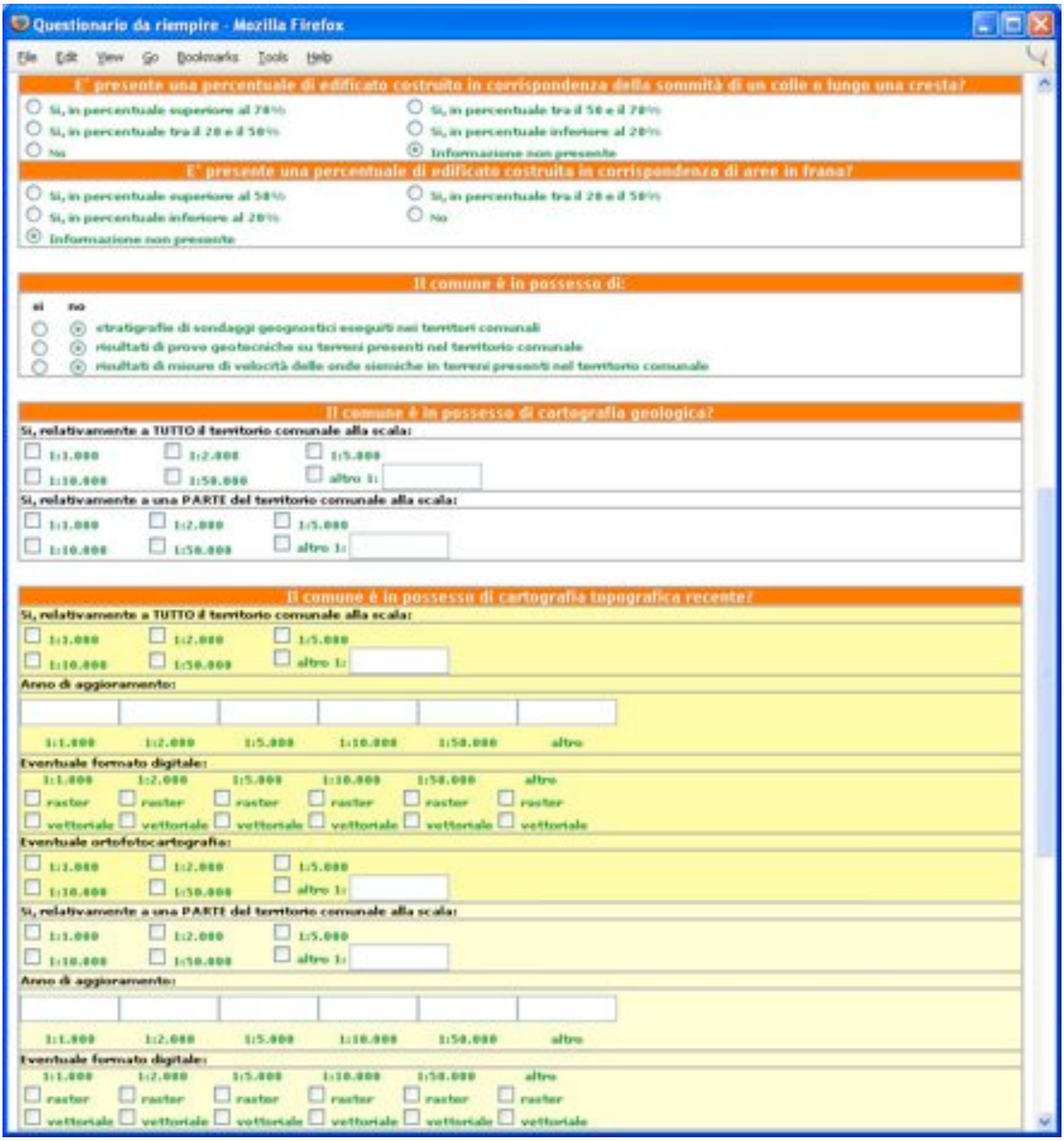

Figure 5.1: continue

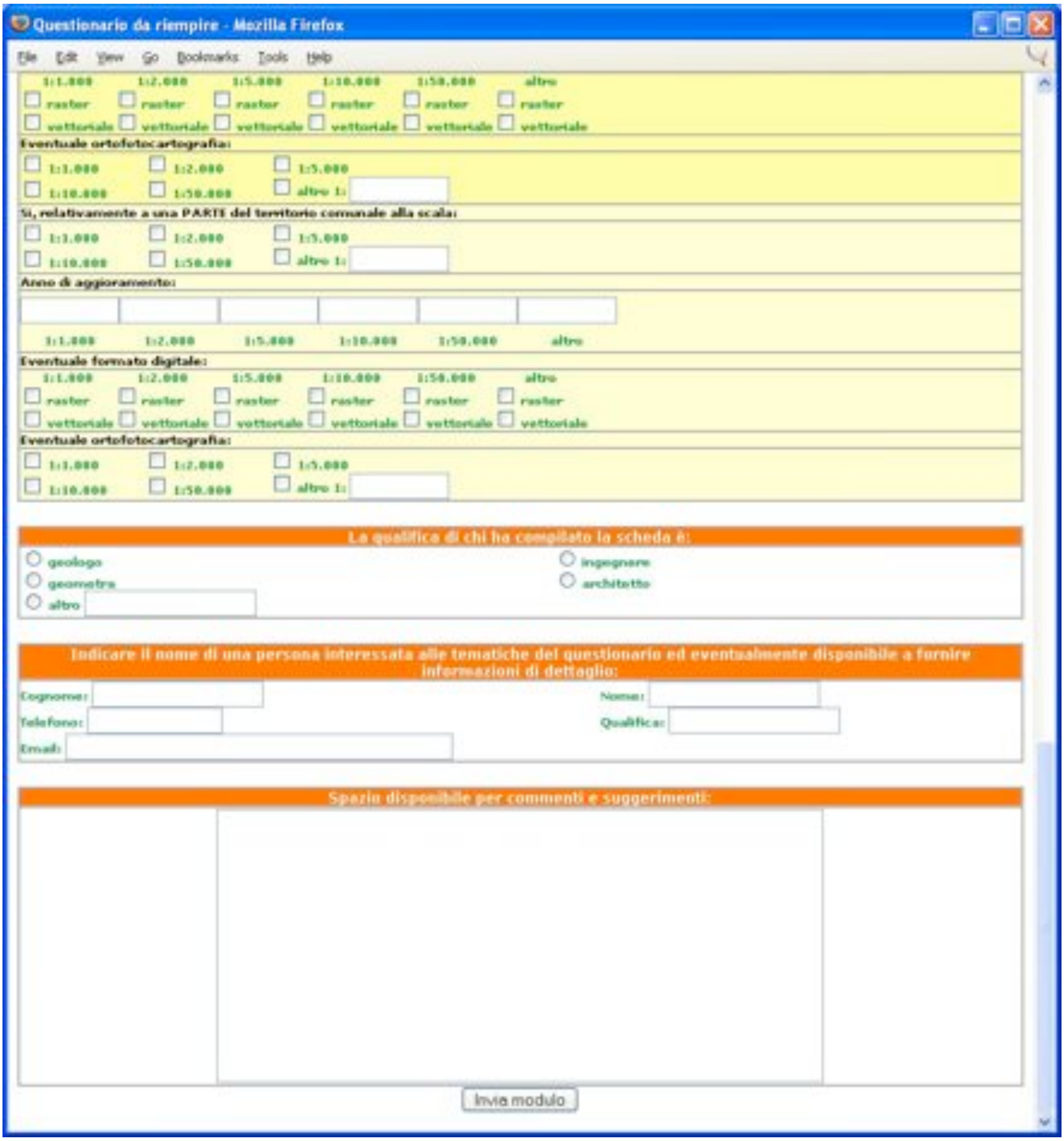

Figure 5.1: continue

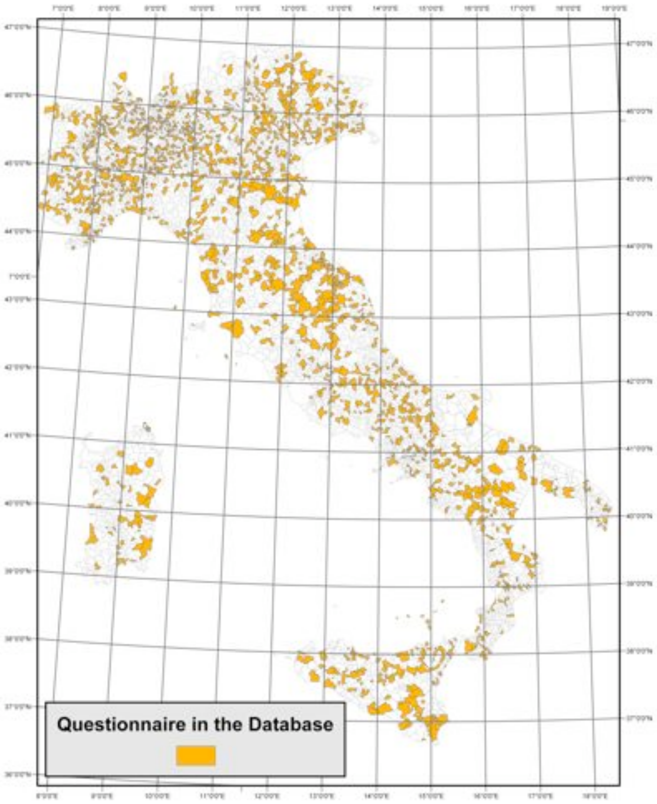

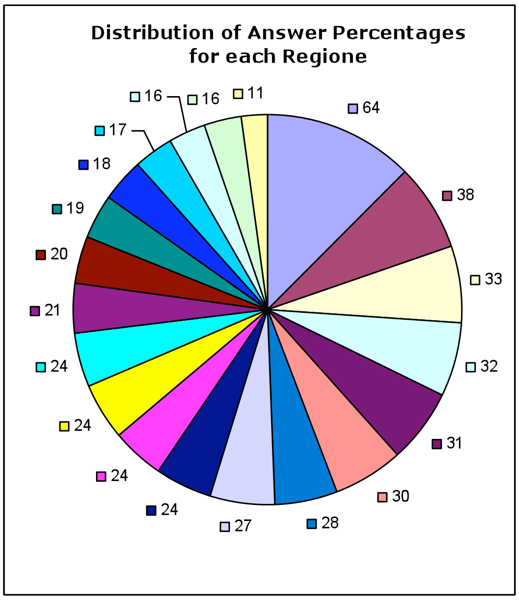

REGION	%
UMBRIA	64
MARCHE	38
TOSCANA	33
BASILICATA	32
VENETO	31
MOLISE	30
LOMBARDIA	28
PIEMONTE	27
VALLE D'AOSTA	24
SICILIA	24
EMILIA-ROMAGNA	24
FRIULI-VENEZIA GIULIA	24
TRENTINO-ALTO ADIGE	21
LIGURIA	20
ABRUZZO	19
CAMPANIA	18
CALABRIA	17
PUGLIA	16
LAZIO	16
SARDEGNA	11

Figure 5.2: For each Region, the picture shows the percentage distribution of answers scaled to the total municipalities

1) Within the Municipality territory, what is the percentage of housing built over the "Rock + Stiff Soil" category and "Soft Soil" category:

Rock + Stiff Soil	0-10%	10-20%	20-40%	40-60%	60-80%	80-90%	90-100%
Soft Soil	90-100%	80-90%	60-80%	40-60%	20-40%	10-20%	0-10%

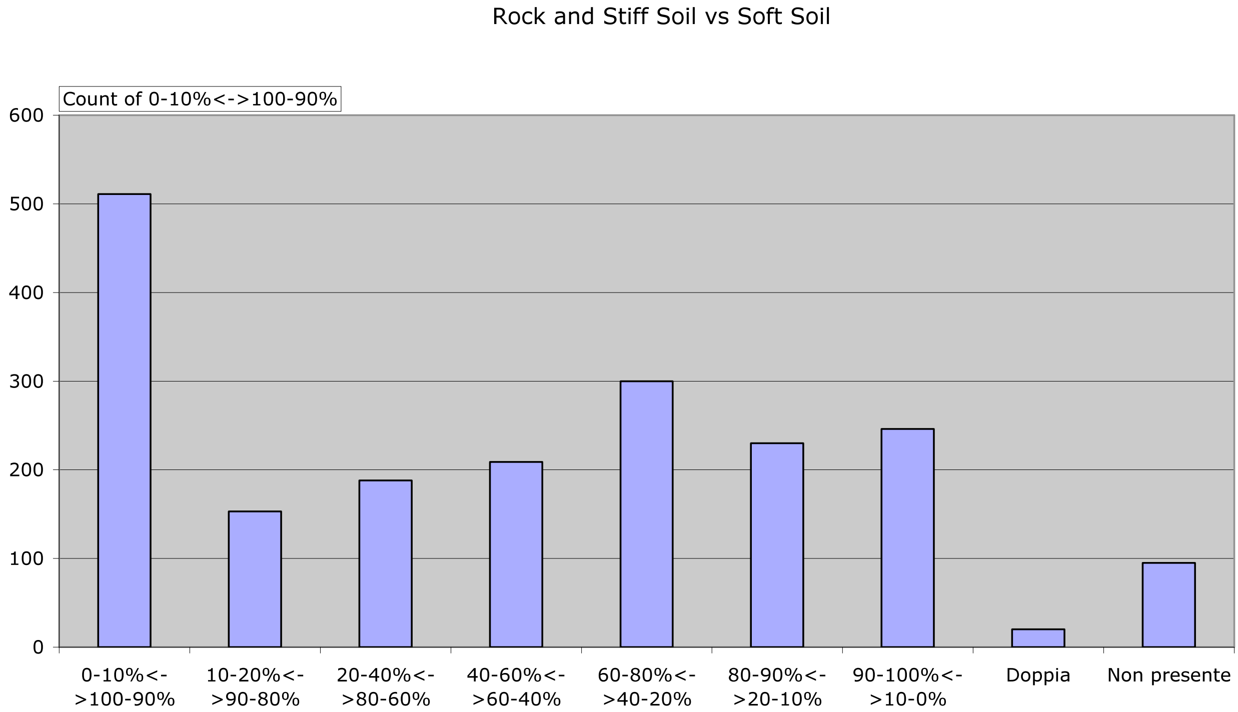

Figure 5.3: Question 1 and the histogram showing the frequency distribution of answer over the seven percentage categories plus a double checking and no answer categories.

2) Of the housing built over the “Rock + Stiff Soil” category, what is the percentage built respectively over the “Rock” category and “Stiff Soil” category

Rock	0-10%	10-20%	20-40%	40-60%	60-80%	80-90%	90-100%
Stiff Soil	90-100%	80-90%	60-80%	40-60%	20-40%	10-20%	0-10%

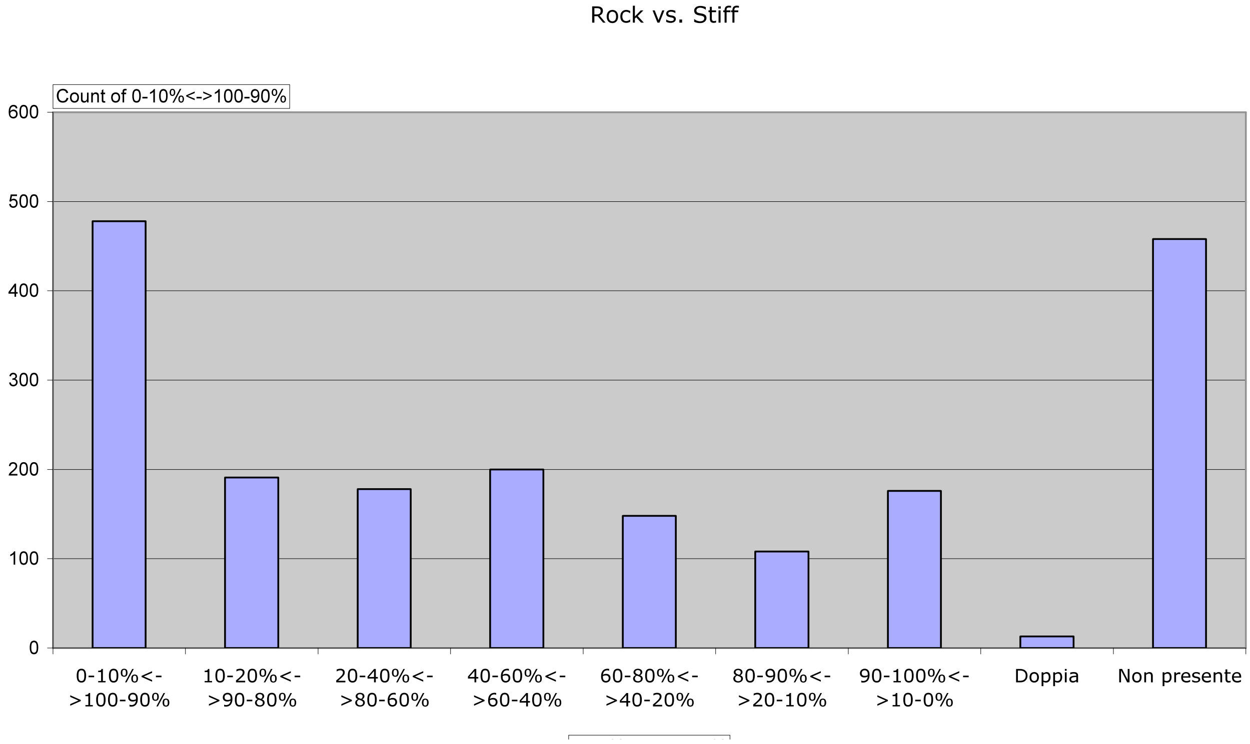

Figure 5.4: Question 2 and the histogram showing the frequency distribution of answer over the seven percentage categories plus a double checking and no answer categories.

3) Of the housing built over soft soil, what is the percentage built on the following "thickness" category:

Thickness >20 m	0-10%	10-20%	20-40%	40-60%	60-80%	80-90%	90-100%
Thickness <20 m	90-100%	80-90%	60-80%	40-60%	20-40%	10-20%	0-10%

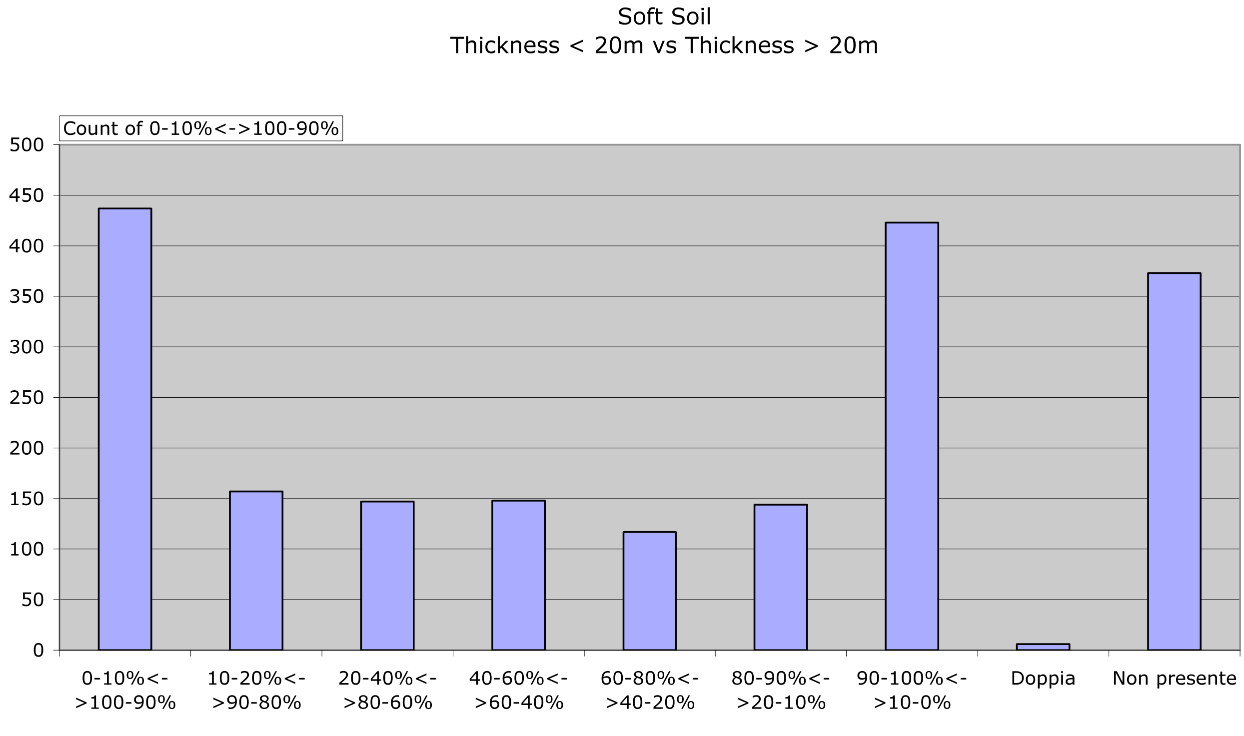

Figure 5.5: Question 3 and the histogram showing the frequency distribution of answer over the seven percentage categories plus a double checking and no answer categories

Figure 5.6: Location of the Municipalities chosen as examples.

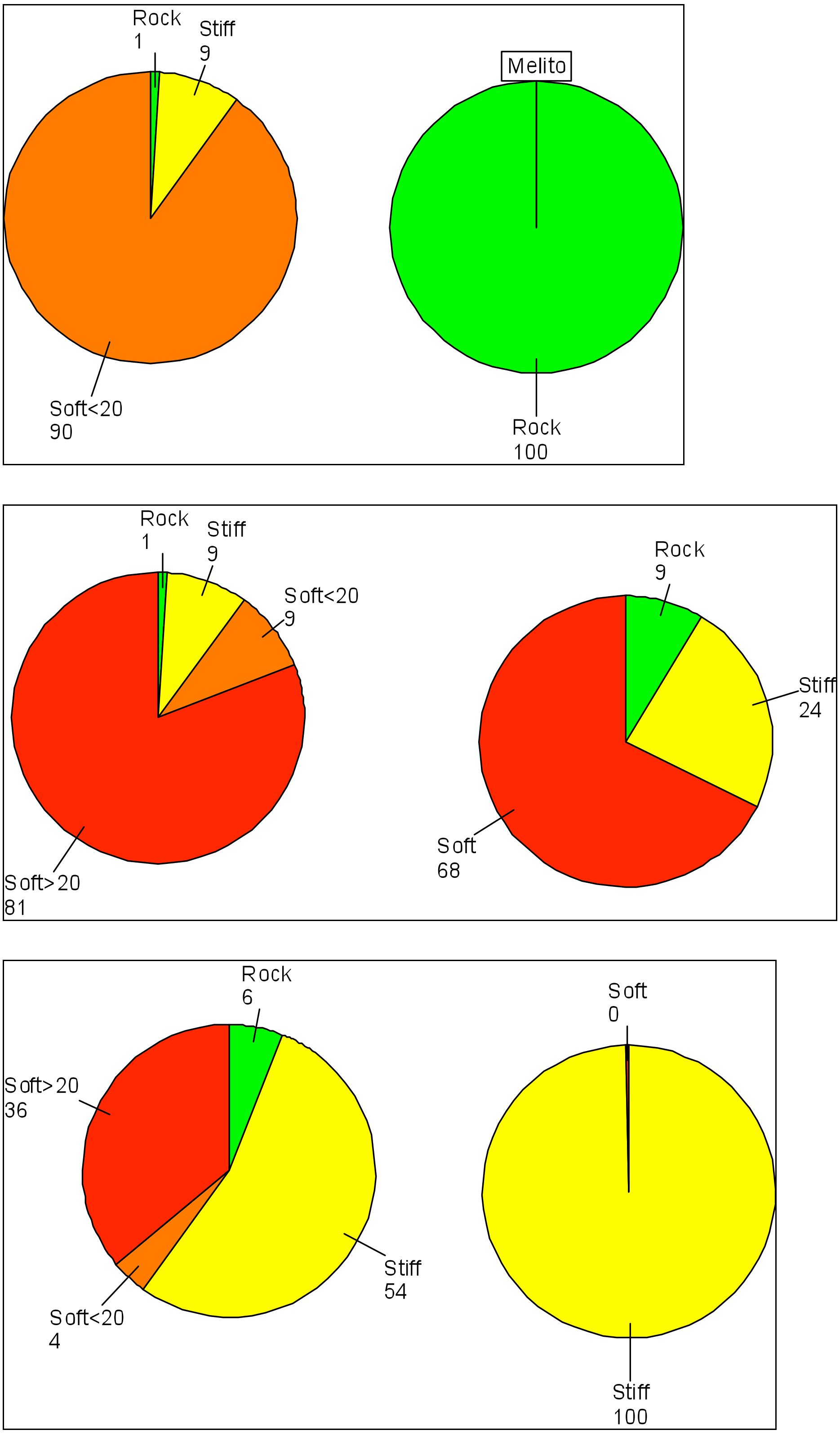

Melito

Fidenza

Istrana

Figure 5.7: Comparison between questionnaire (left hand) and map percentage (right hand). The percentage of the questionnaire is relative to Municipality territory with buildings while the CGM percentage are relative to the whole territory of the Municipality.

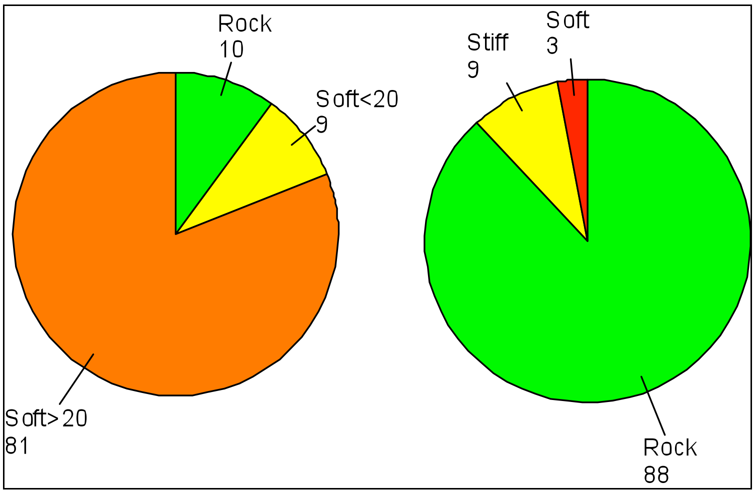

Corato

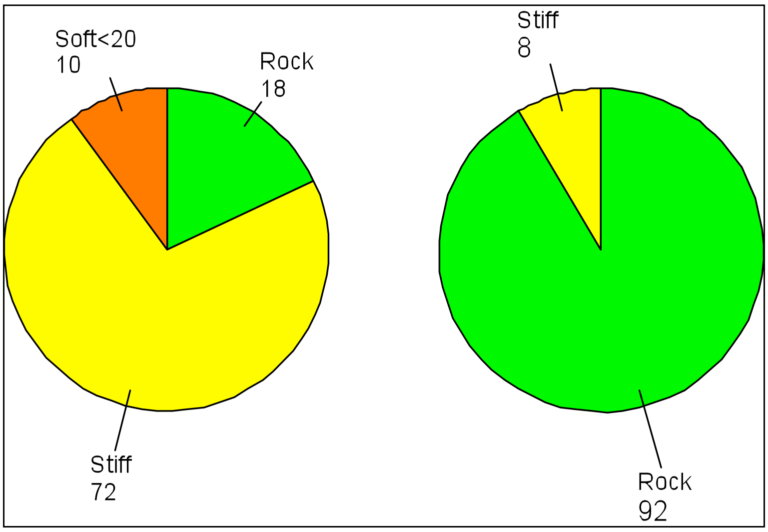

Ampezzo

Figure 5.7: continue